Analysis and Development of Phenomenological Models for the Relative Biological Effectiveness in Proton Therapy

Eivind Rørvik

Thesis for the degree of Philosophiae Doctor (PhD)
University of Bergen, Norway
2019

UNIVERSITY OF BERGEN

Analysis and Development of Phenomenological Models for the Relative Biological Effectiveness in Proton Therapy

Eivind Rørvik

Thesis for the degree of Philosophiae Doctor (PhD)
at the University of Bergen

Date of defense: 23.08.2019

Year: 2019

Title: Analysis and Development of Phenomenological Models for the Relative Biological Effectiveness in Proton Therapy

Name: Eivind Rørvik

Print: Skipnes Kommunikasjon / University of Bergen

«Å leve går an
uten Brann
og uten bauekorps og vannkopper på Haukeland.
Eg e glad i godt ver
og torre kler,
men likevel så sønger eg så ofte så eg kan:

Eg ve te Bergen, ve te Bergen med det samme.
Der har eg det så fisken i vannet:
Vått og kaldt, og breiflabb overalt.»

- *Knutsen og Ludvigsen*

Scientific environment

The PhD study is part of the project «3D microdosimetry and studies of the Relative Biological Effectiveness (RBE) in proton- and carbon ion therapy» funded by the Bergen Research Foundation. The project includes both development of biological models and detector development and is organised by project leader Kristian Smeland Ytre-Hauge within the subatomic physics group at Department of Physics and Technology at the University of Bergen.

The study in this work was aided by dose planners, medical physicists and oncologists at the Department of Medical Physics and Oncology at Haukeland University Hospital (HUH). The department consists of a radiotherapy clinic with active research, performed by researchers/experts within radiation therapy and general medical physics. HUH is planning to build a proton therapy facility within five years.

Parts of this work were also done in collaboration with Monte Carlo experts at Centro Nazionale di Adroterapia Oncologica (CNAO), an operational proton and carbon ion therapy center in Pavia, Italy. One month was spent in Pavia, providing a clinical introduction to particle therapy and practical training.

Acknowledgements

This work was made possible by a generous grant given from Bergen Research Foundation. I am grateful for the opportunity to be a part of the development of the Medical Physics Group at the Department of Physics and Technology and proton therapy research environment in Bergen. Contrary to the myth, the work of this doctoral thesis has not been a solo project, written in total isolation. Therefore, I want to show my appreciation to some people:

First most, I want to thank my supervisor, Dr. Kristian Smeland Ytre-Hauge, for believing in me. I am one of the few lucky PhD students who had daily meetings with the supervisor, which is a rare phenomenon in the academical world. The mix of being able to lead, administer and give feedback to a large group of master's and PhD students, write research grants and articles, teach courses, respond to emails late at night and in weekends, while still having more hours at the end of the day to raise a family, is beyond my understanding. Kristian is going places; University of Bergen is lucky to have him, and I am proud to have been his first PhD student.

A warm thanks to Dr. Sara Thørnqvist at Haukeland University Hospital and her devotion for my work. Her persistence has kept me on track and given me confidence in my results and statistical analysis. The quality and amount of her feedback on my work is far above what is expected. I also thank my other supervisor Dr. Andrea Mairani at HIT/CNAO for helping me understand and write the Monte Carlo codes and the invitation to stay at CNAO.

I want to thank the researchers and staff at Haukeland University Hospital for helping me out with dose planning and clinical know-how: Grete May, Jon Espen and especially Camilla, for showing great interest and giving precious feedback in the process of modelling and writing. I am grateful for the fruitful discussions, spellchecking, code sharing, the hour-long lunch breaks and good times that I have had with my colleagues at IFT: Helge, Andreas, Lukas, Zhuo and especially Lars Fredrik and Tordis!

Thank to my friends in Bergen for bringing lots of joy in the evenings. A special thanks to my brothers for their support through these years. To my mom and dad for their endless love and encouragement; I am privileged to have such parents.

And of course, Helene, thank you for never giving up on me for the last three and half years; you have surely been patiently waiting for me. I'm looking forward to getting rid of my frequent flyer membership and share the whole week together with you in Oslo, not just the weekends. To become your husband will always be my greatest accomplishment.

Abstract

Proton therapy is undergoing a rapid development making it increasingly popular as a treatment of cancer. Protons interact differently with the tissue compared to conventional radiation therapy with photons, resulting in a more beneficial dose distribution with greater dose conformation. The radiation quality is also different for protons and photons, as the ionisation density, often quantified by the linear energy transfer (LET), is higher for protons than for photons. Irradiation experiments on cells and animal models have shown that protons are slightly more effective in producing biological damage than photons. This difference in biological response is quantified by the relative biological effectiveness (RBE), which aid the comparison of the dose deposition from the two modalities and enables transferal of established clinical protocols from photon therapy to proton therapy. A conservative and constant RBE of 1.1 is used in proton therapy clinics, even though experiments have shown that the RBE can be both higher and lower, varying with different biological and physical quantities, including the LET value.

Phenomenological RBE models try to determine the various RBE dependencies from large experimental databases of cell irradiation experiments. In this work, existing phenomenological models were analysed and explored in a coherent manner: All models were parameterised and described by functions of the maximum RBE (RBE_{max}) and minimum RBE (RBE_{min}), the two model functions that make every model unique. The models were implemented in the FLUKA Monte Carlo code and used in estimation of the RBE and RBE-weighted dose for multiple patient plans and relevant dose parameters. The models were also analysed and compared regarding the underlying similarities and differences, which forms the basis for the unique definitions of RBE_{max} and RBE_{min} of each model. A new phenomenological RBE model was proposed, introducing the full LET spectrum as an input parameter for phenomenological models. Statistical methods were used to test whether a non-linear LET dependency of RBE_{max} would give a superior description of the experimental data compared to using the established linear dependency of the dose-averaged LET (LET_d). Further, we analysed the LET_d dependency of RBE_{min} in a two-step regression analysis, as the RBE_{min}

function is most commonly assumed to be constant for all LET_d values. Specifically, we analysed how restriction on the minimum dose of the underlying experimental database influenced RBE_{min}.

The estimation of the RBE and the RBE-weighted dose from the various models differed significantly. The largest deviations were seen for organs at risk (OAR) with low fractionation sensitivity ($(\alpha/\beta)_x$) and high LET. These variations are a result of the distributions of $(\alpha/\beta)_x$ values and LET_d values in the experimental databases, the assumptions for RBE_{max} and RBE_{min} and regression analysis method. The full LET spectrum was found to give a better representation of the experimental database included in our analysis. Regression weighted to the reported experimental uncertainties showed that a non-linear function (quartic function) gave a better fit to the data than a linear function. The RBE_{min} function was found to vary with the LET_d value if dose constraints were added to the experimental database. By restricting the minimum dose in the database to be 1 Gy or lower, the analysis gave a non-negligible linear LET_d dependency, while higher minimum doses indicated that the dependency is constant.

The deviations in the estimated RBE from the models can be traced back to the model differences in the database construction, the model assumptions and the regression techniques. Various methods were used in this thesis to develop novel models by reanalysing published data, such as construction of model databases with strict constraints, using the pure dose-survival data instead of only α and β values, statistical analysis of model assumptions, applying multiple regression techniques and recognition of the LET spectrum as a relevant input parameter. Together, these techniques could minimise the researcher bias and make more accurate RBE models, resulting in better dose predictions for clinically relevant scenarios.

List of Publications

Papers included in the thesis

Paper I: Rørvik E, Fjæra LF, Dahle TJ, Dale JE, Engeseth GM, Stokkevåg CH, Thörnqvist S, Ytre-Hauge KS. (2018) *Exploration and application of phenomenological RBE models for proton therapy*. Physics in Medicine & Biology 63(18), p185013

Paper II: Rørvik E, Thörnqvist S, Stokkevåg CH, Dahle TJ, Fjæra LF, Ytre-Hauge KS. (2017) *A phenomenological biological dose model for proton therapy based on linear energy transfer spectra.* Medical Physics 44(6), p2586-2594

Paper III: Rørvik E, Thörnqvist S, Ytre-Hauge KS. *The experimental dose ranges influence the LET_d dependency of the proton minimum RBE (RBE_{min}).* Submitted to Physics in Medicine & Biology

Conference presentations

Rørvik E, Ytre-Hauge KS. *Utilization of Linear Energy Spectra to Estimate the Relative Biological Effectiveness in Proton Therapy*. MEDFYS 2016, February 2016, Kvitfjell, Norway (Poster)

Rørvik E, Ytre-Hauge KS. *A Model for the Relative Biological Effectiveness for protons based on the Linear Energy Transfer Spectrum*. ICTR-PHE 2016, Februar 2016, Geneva, Switzerland (Poster)

Rørvik E, Fjæra LF, Dahle TJ, Søbstad JM, Stokkevåg CH, Thörnqvist S, Ytre-Hauge KS. *A Comparison of Phenomenological RBE Models in Proton Therapy*. NACP 2017, Februar 2017, Oslo, Norway (Poster)

Rørvik E, Thörnqvist S, Ytre-Hauge KS. *Higher Biological Dose to Heart and Lung in IMPT of Medulloblastoma Patients Due to Increased LET*. ESTRO 2017, May 2017, Vienna, Austria (Poster)

Rørvik E, Thörnqvist S, Ytre-Hauge KS. *Is the Beta Parameter of the Linear Quadratic Model for Cell Survival Decreasing or Increasing with the Linear Energy Transfer of Protons?* MEDFYS 2018, Februar 2018, Kvitfjell, Norway (Poster)

Rørvik E. *Scoring of Linear Energy Transfer (LET) for Calculation of Biological Dose in Proton Therapy.* 4th Fluka Advanced Course and Workshop 2016, May 2016, Paris, France (Oral presentation)

Rørvik E, Fjæra LF, Dahle TJ, Dale JE, Engeseth GM, Stokkevåg CH, Thörnqvist S, Ytre-Hauge KS. *Variation in Biological Dose Estimates Among Phenomenological RBE Models for Proton therapy.* BIGART 2017, June 2017, Aarhus, Norway (Oral presentation)

Thörnqvist S, Ytre-Hauge KS, Rørvik E. *The experimental dose ranges influence the LET dependency of the proton minimum RBE*. PTCOG 58, June 2019, Manchester, England (E-poster discussion)

Additional papers co-authored, not part of the thesis

Stokkevåg CH, Fukahori M, Nomiya T, Matsufuji N, Engeseth GM, Hysing LB, Ytre-Hauge KS, Rørvik E, Szostak A, Muren LP. (2018) *Modelling of organ-specific radiation-induced secondary cancer risks following particle therapy*. Radiotherapy and Oncology 120(2), 300–306

Dahle TJ, Rykkelid AM, Stokkevåg CH, Mairani A, Görgen A, Edin NJ, Rørvik E, Fjæra LF, Malinen E, Ytre-Hauge KS. (2017) *Monte Carlo Simulations of a Low Energy Proton Beamline for Radiobiological Experiments*. Acta Oncologica 56 (6), 779–786

Contents

1. Introduction

Cancer is a group of diseases where the genetic code of a cell has mutated, leading to an abnormal cell growth with the potential of also invading other regions of the body. From being an almost certain death 50 years ago, the development of better diagnostics and treatment through cancer research have changed the face of cancer. Overall survival rates for cancer diseases have been steadily increasing since the 1970s (Quaresma, Coleman, and Rachet 2015). A study assumed that approximately 5 million have avoided death to cancer in Europe over the three last decades (Malvezzi et al. 2018). Still, at what might seem contradictive, cancer was the most common cause of death in Norway in 2017 for the first time (FHI 2018). It is estimated that over 30 000 patients every year are diagnosed with cancer in Norway, and the number is increasing.

Radiation therapy is one of three main modalities used for cancer treatment, together with surgery and chemotherapy. A study reported that around half of all cancer patients in Australia would benefit from radiation therapy (Barton et al. 2014). The principle of radiation therapy is that ionising radiation should target and damage the unwanted cancer cells, while sparing the healthy normal cells. If the treatment is successful, the cells are not able to proliferate, and the cancer cells will eventually die.

As more people are cured from cancer, an increasing amount of people are also living with complications and late reactions induced by the radiation therapy. The damage to the healthy tissue should be minimised to avoid harming the patient. There exists therefore a strong rationale for decreasing the dose to the non-cancerous tissue of patients, as one assumes there is a correlation between higher dose and increased normal tissue complication probability (NTCP).

Today, conventional external radiotherapy is delivered by linear accelerators, creating high energetic X-rays that penetrate through the body, harming cells on the way through the patient. Radiotherapy have been aided heavily by modern technology and software development over the last decades. The radiotherapy technology has taken incremental steps to optimise the treatment delivery; from simple single field plans all the way to complicated Volumetric Modulated Arc Therapy (VMAT) plans. Every step

has increased the overall dose conformity, targeting tumour tissue and sparing healthy tissue. However, the steady increase in dose conformity through technological developments is about to converge towards a physical limit, governed by the spatial dose distribution of photons and electrons. For many sites, organs at risk (OAR) still limit the dose that can safely be administered to the target volume. Conventional photon treatment may deliver an unacceptable large dose to OAR, due to the physical dose distribution of photon beams.

If the patient is treated with protons instead of photons, the dose conformity in radiation therapy can still be improved. A proton beam has a significantly different depth dose curve compared to photons. High energetic X-rays and gamma-rays have a depth dose distribution with a maximum a few centimetres into the tissue and thereafter decreasing with increasing depth. Protons on the contrary have a relative flat dose in the entrance and a maximum towards the end of their path, known as the Bragg peak. The location of the Bragg peak is determined by the energy of the proton beam. This energy can be modulated to create a spread out Bragg peak (SOBP), which cover the full extent of the tumour with a uniform dose (Wilson 1946).

The number of patients treated with proton therapy is increasing at an exponential rate, with a more than 170 000 patients treated worldwide (Jermann 2018). In general, the better dose conformity of protons compared to conventional radiation lowers the dose to OARs and other normal tissue, which will lower the NTCP for many patients (Widder et al. 2016). However, the increased dose conformity is not the only benefit from protons.

The ionisation density of protons is higher than for photons, meaning that ions are more effective in the inactivation processes of cancer cells. If photons and protons deliver the same physical dose, the latter will be more biological effective, e.g. inactivate a higher fraction of cells. This difference is not negligible and must be accounted for in proton therapy. The relative biological effectiveness (RBE) is introduced as a scaling factor for the physical proton dose. The quantity is able to estimate the comparable photon doses to proton doses, consequently aiding the transferral of knowledge gained

from photon therapy to proton therapy. Based on experiments with animals in the 1970s, the RBE of protons was set to be 1.1, i.e. protons are assumed to be 10% more effective than photons for the same physical dose. The conservative value is still used today in proton therapy clinics, even though experiments have shown that the RBE can be higher and varies with the fraction dose, tissue type and the ionisation density. Multiple dose planning studies of patient plans have shown that a potential variable RBE could lead to an increased dose to OARs compared to the doses reported by the clinically used treatment planning system, which only calculate the dose using an RBE of 1.1. These studies estimated RBE from various RBE models. Phenomenological RBE models are a group of models that rely and focus on experimental data. The model creators try to find relationships between the input and output quantities of experiments without modelling specific subcellular effects, contrary to mechanistic models.

The goal of this study was to analyse and compare established phenomenological RBE models for proton therapy, by exploring their similarities and experimental basis. We also wanted to investigate existing experimental data found in the literature to develop novel phenomenological models. The creation of better and more precise RBE models could improve the dose determination of proton therapy and make safer and better predictions of the treatment outcome.

2. Radiation physics

Ionising radiation is radiation that carries high enough energy to ionise material, i.e. removing electrons from atom and molecules. The treatment dose in radiotherapy is traditionally quantified using the absorbed dose, D, representing the amount of energy deposited by the radiation per unit mass of the tissue:

$$D \equiv \frac{\Delta E}{\Delta m}, \tag{2.1}$$

where ΔE is the energy (Joules) and Δm is the mass of the tissue (kg) where the energy is deposited. The absorbed dose is a physical measurable quantity, measured in units of Gray (Gy). Conventional radiation therapy is performed by neutral photons without mass, whereas proton therapy is performed with massive charged particles. The primary goal of radiation therapy is to damage the DNA molecules inside the cancer cells, either directly by the initial particles/radiation (direct action) or subsequently by free radicals produced by the radiation (indirect action). The biology is further described in section 3, while an overview of the physical interactions between protons and tissue are given in this section.

2.1 Proton Interactions

The protons are accelerated to relativistic velocities before entering the patient. They will primarily interact with the patient's tissue through three different mechanisms: Stopping, scattering and nuclear interactions. Bremsstrahlung is also theoretical possible, however, at therapeutic proton energies the effect is negligible (Newhauser and Zhang 2015).

When the protons traverse the tissue, electrons will absorb parts of the kinetic energy through electromagnetic force interactions, resulting in ionisations and excitations. As a result, the kinetic energy of the protons is transferred to the matter and the protons are slowed down. This inelastic force imparted on the protons from the matter is termed "stopping power" and defined as the loss of energy per unit of length. The force is dependent on multiple parameters, such as the material composition and electron density of the tissue and the velocity of the protons. The stopping power for different

charged particles and materials can be calculated by the Bethe-Bloch formula (Bethe 1930, Bloch 1933a, 1933b) or experimental tables (Lühr et al. 2012, Greilich et al. 2010, ICRU 1993). The protons will ionise the impacted molecules and create secondary electrons (delta ray), transferring energy from the protons to the material. This is described more in depth in section 2.3.

In addition to being stopped by the electrons in the tissue, protons also interact with the electromagnetic field of the nuclei. If the protons come too close to the nucleus, the protons may change their trajectory, introducing a lateral deflection in the proton track. The elastic coulomb interactions between the protons and the nuclei are dependent on the charge of the nuclei, which can be analytical calculated by the Molière's theory (Molière 1948, Bethe 1953). Heavier elements in the tissue will increase the magnitude of scattering. Beam absorbers should therefore be created of material with low Z, to decrease the spread of the pencil beam (Brennsæter 2015).

The electromagnetic interactions with the electrons and the nuclei of the tissue material are the dominating modes of interaction, however, in rare instances, protons are also able to overcome the Coulomb barrier and interact directly with the particles within the nucleus. These nuclear interactions can result in secondary particles through creation of heavier elements and recoil particles from the tissue, which themselves can ionise the tissue (Paganetti 2002). Similar to the ionised electrons, these secondary particles can be highly energetic and interact with tissue far away from the central axis of the protons, by creating delta rays or ion clusters. Besides secondary protons, helium ions are the most usual secondary particles seen in proton therapy. These are primarily created in the entrance, when the kinetic energy of the proton beam is high (Grassberger and Paganetti 2011, Paganetti 2002).

The three different interactions describe the energy transfer on a subatomic scale between the proton and the tissue. All these interactions can be regarded as random and stochastic, even though the probability of an interaction is dependent on the proton energy, electron density and nuclei composition in the tissue (Newhauser and Zhang 2015). The stochastic nature of every interaction makes it impossible to predict the fate

of a single proton, and every proton track and local dose deposition is unique. A schematic example of a short proton track is shown in the diagram in Figure 1A.

2.2 Macroscopic dose distrubution

In a clinical beam, billions of protons are accelerated and used in the irradiation of the tumour. The beam consists of many independent track structures. This leads to a stable and reproducible dose distribution, following the mathematical laws of large numbers (Metropolis and Ulam 1949). A macroscopic dose distribution of a monoenergetic proton beam deposited in a water phantom is illustrated by isodose curves in the lateral direction in Figure 1B and the dose intensity along the central axis in Figure 1C.

The ionisation density of the traversing protons increases towards the end of the range, before the protons come to a halt. This results in the distinctive peak at the end of the depth dose distribution. The initial energy spread in the proton beam combined with the stochastic nature of the proton stopping (i.e. range straggling) determine the width of the Bragg peak. The scattering effect is significant in proton therapy compared to heavier ions, and narrow pencil beams will broaden and become widened at the end of range, as seen by the expanded isodose curves in Figure 1B.

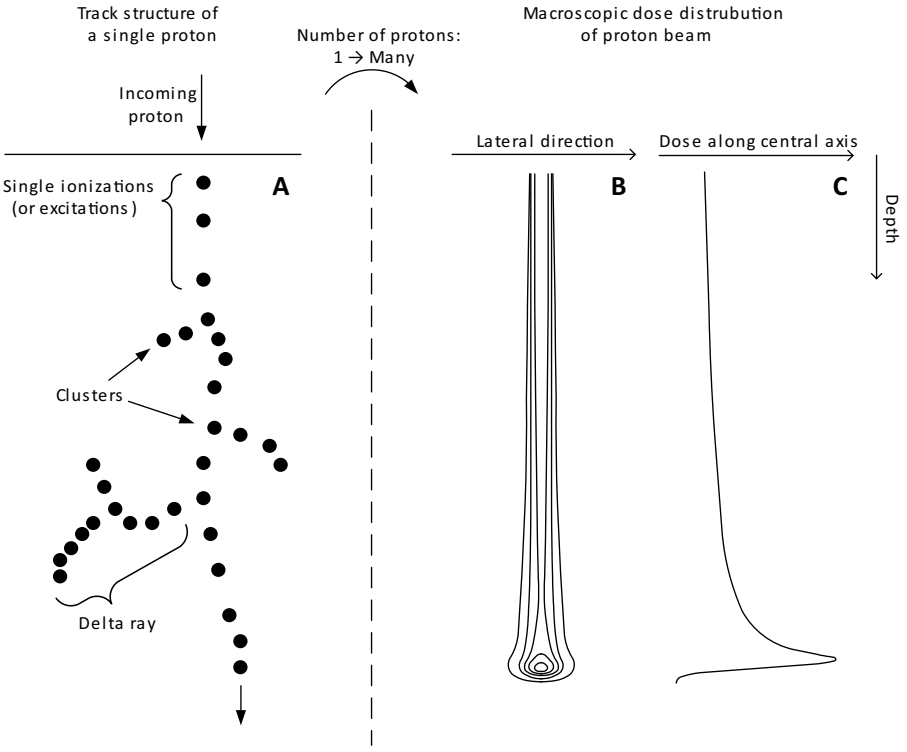

Figure 1: A: An example of the track structure in a nanometric scale of an accelerated proton traversing matter. Each point represents one interaction between the traversing proton or secondary particles and the atoms in the tissue. Although a single-track structure is chaotic, many protons leads to a stable dose distribution, as shown in the macroscopic diagrams in B and C. B: Arbitrary isodose curves, illustrating the result of lateral scattering, i.e. a broadening of the lateral dose with depth. C: The depth dose distribution along central axis, where the dose is relatively constant until the distinctive Bragg peak. Inspired by ICRU report 16 (1970).

2.3 Linear energy transfer

Even though two different radiation modalities, e.g. 6 MV photons and protons, deposit the same physical macroscopic dose within the tissue, the pattern of dose deposition can be different because of differences in the ionisation density and track structure. The term radiation quality is used to describe these physical properties, normally quantified by the linear energy transfer (LET) of the radiation (ICRU 1970). LET is defined as

the infinitesimal amount of mean energy transferred from the proton to the tissue locally (dE in keV) per infinitesimal part of the proton track (dl in µm):

$$LET = \frac{dE}{dl}. \tag{2.2}$$

The energy transferred to the tissue locally from a proton could maximum equal the energy lost by the proton. If the energy of the incoming proton is high enough, the collision could create delta ray electrons, which could deposit their energy relative far away from the origin. A restricted LET (LET_Δ) definition is used to focus on the energy deposited in the vicinity of the proton track, which exclude the transfer to electrons with energies above a maximum transfer energy Δ. If all collisions are included in the definition, the quantity is termed unrestricted LET (LET_∞). As no energy is excluded, LET_∞ will then equal the stopping power of the proton. There is little difference between LET_Δ and LET_∞ in the clinical energy range for protons and relevant secondary particles (Grzanka 2014).

The LET is dependent on the energy of the traversing proton, as the stopping power varies with the velocity of the proton. As shown in Figure 2, the LET value decreases with increasing energy and ranges between 0.2 and 84 keV/µm in the clinical relevant energy range (ICRU 1993, Wilkens, J J and Oelfke 2004). By integrating the proton stopping power from zero to the full proton energy, the residual range of the proton can be estimated, e.g. by the continuous slowing down approximation (CSDA) (Fano 1953). As shown, the LET value increases with decreasing CSDA, i.e. closer to the proton track end.

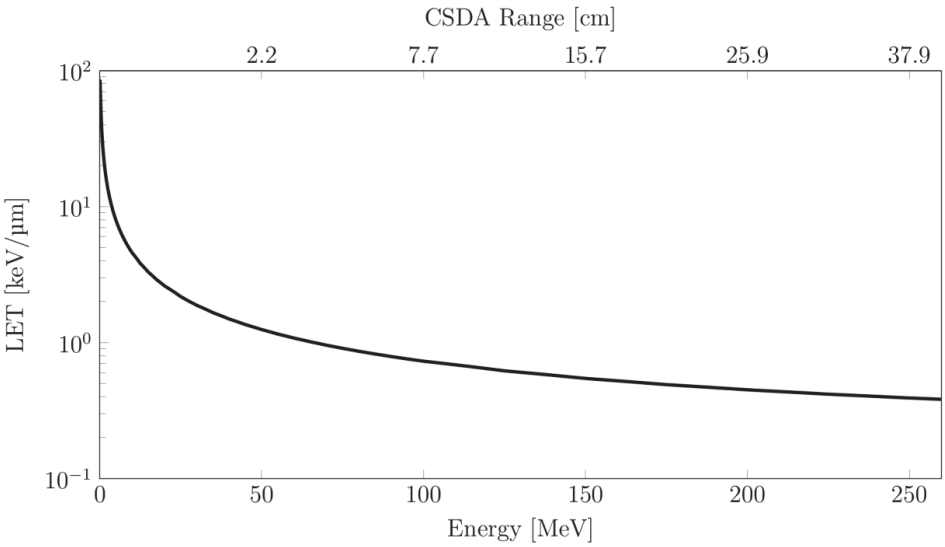

Figure 2: The unrestricted LET value of protons in water as a function of the energy of the proton. The x-axis on the top quantifies the remaining range of the protons in water, estimated with the continuous slowing down approximation (CSDA). The curve was obtained using the Libamtrack online calculator (Greilich et al. 2010).

The LET value also varies significantly the type of particle traversing the tissue, as heavier particles such as helium and carbon ions have a higher electrical charge, leading to a greater stopping power. Furthermore, the stopping power is dependent on the electron density and the composition of the tissue material with different materials leading to a change in the LET value of the accelerated protons (Bernard Gottschalk 2011). In conventional photon therapy, the dose is reported by the dose to water (D^w) instead of the dose to tissue. Similarly, radiation quality is primarily reported by the LET to water (LET^w), independent on the tissue the particles are traversing through (Wilkens, Jan J. and Oelfke 2004, Paganetti 2009).

For an infinitesimal volume, the dose from monoenergetic protons can be calculated from the fluence and the LET value of those protons:

$$D = \frac{\theta}{\rho} LET, \tag{2.3}$$

where θ is the proton fluence and ρ is the tissue density. As the equation states, fewer protons are needed to deposit a prescribed dose for a beam consisting of high LET

protons, compared to a beam consisting of low LET protons. Equation (2.3) can also be used to describe the dose to water, by finding the LET^w from tables and using the water density (ρ^w) instead of the specific tissue density.

2.3.1 Linear energy transfer spectrum

In a clinical setting, the treatment beam within the patient do not consist of only monoenergetic protons, even for pristine pencil beams. As the mean energy decreases with increasing depth, the energy spread increases and the stochastic nature of stopping and scattering creates a beam with a range of energies. In addition, heavier secondary particles are produced by nuclear interactions and "pollutes" the proton beam (Grassberger and Paganetti 2011). The radiation quality can therefore be described by a dose weighted spectrum from protons of different LET values (d(L)) at every spatial location, instead of a single quantity:

$$\int_0^\infty d(L)\, dL = \frac{1}{D}\int_0^\infty D(L)\, dL = 1, \tag{2.4}$$

where L is the LET value, D(L) is the absolute dose yielded by particles with LET value L and D is the total dose given to the specific location. The dose weighted LET spectrum (d(L)) is defined such that the sum of all dose compositions is normalised to 1 (ICRU 1970).

Examples of dose weighted spectra are shown in Figure 3, where the LET spectrum is depicted in the entrance and at the Bragg peak. As shown, the spectrum is narrow in the entrance, while at the end of the range the spectrum is shifted towards higher values and broaden out. The composition of the beam gets increasingly complex for a Spread-out Bragg Peak (SOBP) beam with multiple initial energies, and even more complex for treatments with many fields, often termed a "mixed treatment field" (Lam 1987, Inaniwa et al. 2015).

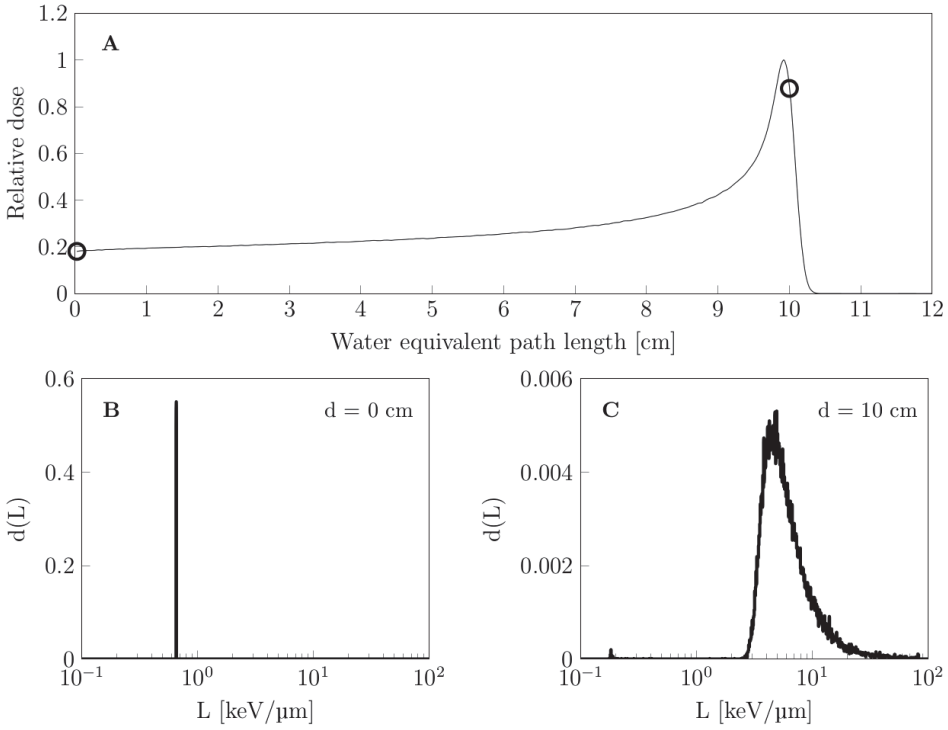

Figure 3: A depth dose curve of a monoenergetic proton beam of 116 MeV in a water phantom shown in Figure A. The LET spectrum at the entrance is shown in B and the spectrum at the Bragg peak is shown in C, both positions illustrated in A. The depth dose curve and the LET spectra is created by the author with the FLUKA Monte Carlo code.

Alternatively, the LET spectrum can be track (or fluence, f(L)) weighted , where the LET values are distributed relative to the number of particles traversing the tissue instead of the dose deposited by them. For our work, we only focus on the dose weighted LET spectrum, hereafter referred to as the LET spectrum. For simplicity, it is common to only use the dose averaged LET (LET_d) value, a single quantity, instead of the full LET spectrum (Polster et al. 2015):

$$LET_d = \int_0^\infty L\, d(L)\; dL = \frac{1}{D}\int_0^\infty L\, D(L)\, dL. \tag{2.5}$$

Generally, the LET_d value increases with increasing treatment depth, and the highest LET_d values are found distal to the Bragg peak at the distal dose falloff. In a practical clinical setting, only a limited range of LET_d values between 0 and 20 keV/µm are seen

(Paganetti 2014). The typical LET_d values in the middle of the SOBP, i.e. middle of the tumour, are 2-3 keV/µm.

Alternative approaches to describe the radiation quality are the energy spectrum (Belli, Campa, and Ermolli 1997) or microdosimetric quantities such as lineal energy (l) or specific energy (z) (Loncol et al. 1994, Inaniwa et al. 2010) or the number of proton pencil beam track-end (Traneus and Ödén 2019).

3. Radiation biology

The purpose of radiation therapy is to heal cancer patients by sterilising and stopping the proliferation of the cancer cells. Studies have shown that the DNA within the nucleus is the molecule target which inactivates the cancer cells, as well as normal cells (Kaplan and Moses 1964). The ionisation process might lead to single strand breaks (SSB) or double strand breaks (DSB) of the DNA molecules. Most SSB are repaired immediately or at most a few hours later by biological processes (Hall and Giaccia 2006). Incomplete repair of the damaged DNA might induce cell death, inhibiting the proliferating of cells. Generally, normal cells have lower division rates and better repair mechanisms compared to cancer cells, making them more resistant to radiation. In very rare instances the repair can be performed incorrectly and introduce a gene mutation which will be inherited by the daughter cells.

As mentioned in section 2, the DNA can be damaged either directly by the proton beam or secondary electrons, or indirectly by free radicals created in the water around the DNA molecule (Joiner and Kogel 2016). Direct action creates more DSBs than indirect action and is more prominent in proton therapy compared to conventional therapy, as the local ionisation density of a proton beam is higher than for conventional photon radiation (Hirayama et al. 2009).

The biological effects of radiation can be quantified with respect to different endpoints. At the cellular level, endpoints such as e.g. cellular survival, induction of radiosensitive proteins or DSBs, can be measured in cells radiated *in vitro* (Tommasino and Durante 2015). Examples of endpoints for mice and rats irradiated *in vivo* are early skin damage or crypt regeneration (Paganetti et al. 2002). However, clinically the primary and most important endpoints are the tumour control and a variety of normal tissue complications, which forms the basis for the clinical treatment protocols (Hall and Giaccia 2006). These are, however, more complex and difficult to measure, requiring and large clinical trials to be determined.

3.1 The linear-quadratic model

The linear quadratic model (LQ-model) is a general dose response model which can describe the effect of radiation on multiple endpoints, both clinical and pre-clinical. To describe the survival fraction of cells irradiated *in vitro*, the model is defined as:

$$S(D) = \frac{N(D)}{N_0} = e^{-(\alpha D + \beta D^2)}, \tag{3.1}$$

where S is the fraction of cells surviving the radiation, $N(D)$ and N_0 are the absolute number of surviving radiated and non-radiated reference cells and α and β are the LQ-model parameters. The model parameters are found by regression fitting to experimental data. Even though the model coefficients do not have a direct interpretation, the parameters can be coupled to the repair mechanisms of the cells. The first term of the exponential function in Equation (3.1) describes unrepairable lethal damage, while the second term describes the repairable non-lethal damage. The ratio between the parameters (α/β), is commonly used to describe the fractionation sensitivity of different tissues and organs, as it is possible to extract the ratio from clinical endpoints, not only cell survival data. The LQ-model is illustrated in Figure 4 by two survival curves drawn using LQ-model regressions. The LQ model can be expanded to consider other effects that cannot be described by only two parameters. These effects include hyper sensitivity at low doses, linear effects at high doses, hypoxia, time dependencies and repopulation of the cells.

3.2 Relative Biological Effectiveness

By moving from photon therapy to proton therapy, the radiation quality changes, as described in Section 2.3. If the same amount of physical dose is given with photon and proton therapy, the latter will normally have higher effect, i.e. in a cell experiment the proton radiation would have inactivated a higher fraction of the cells (Paganetti 2014).

The variations in biological effect for the same physical dose is described by the relative biological effectiveness (RBE), a scaling factor defined as:

$$RBE = \frac{D_x}{D_p}\bigg|_{\text{iso effect}}, \tag{3.2}$$

where D_x and D_p are the absorbed physical doses deposited by the reference photon and proton radiation, respectively. The RBE can be found by calculating the ratio of the dose levels for a specific endpoint, where both modalities are isoeffective. The most common endpoint measured by RBE experiments is cell survival fraction from *in vitro* irradiation, which also has become the basis for most RBE models. Mathematically, the survival fraction for both radiation modalities equals each other:

$$S(D_p) = S(D_x), \tag{3.3}$$

where $S(D_p)$ and $S(D_x)$ are the survival fractions of proton and photon irradiations, respectively.

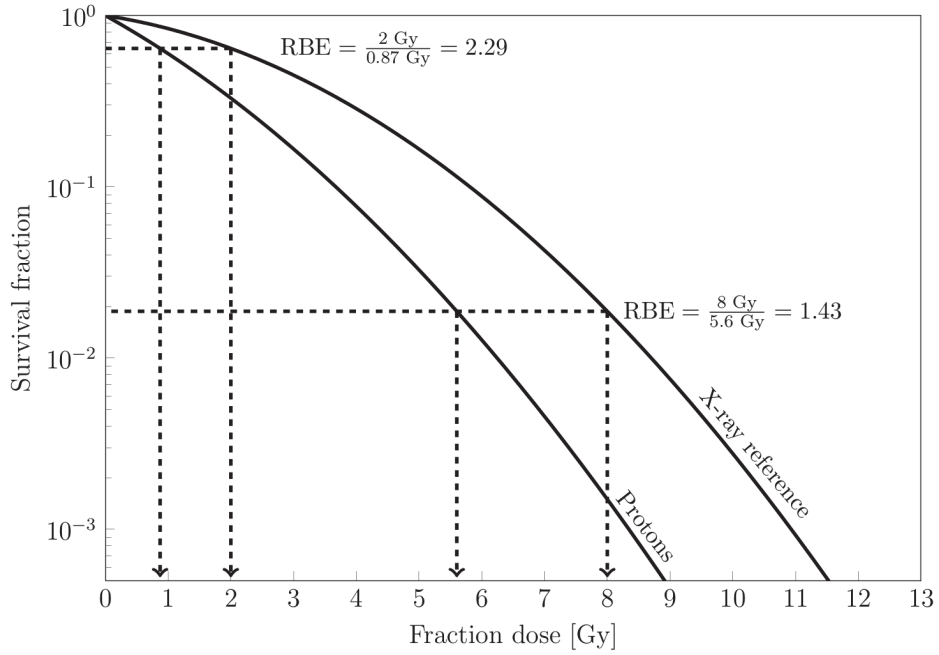

Figure 4: Schematic dose response curves of V79 hamster cells, irradiated with monoenergetic protons (α = 0.469 Gy^{-1} and β = 0.043 Gy^{-2}) and with X-rays (α = 0.129 Gy^{-1} and β = 0.046 Gy^{-2}) as reference radiation. The data originates from Belli et al. (1998).

In vitro and *in vivo* experiments have shown that the RBE is variable and dependent on the measured biological endpoint, cell type, dose and radiation quality. The effect of selected endpoint is visualised in Figure 4. The scientific community, however, agreed in the 1970s that the proton RBE can be regarded as constant and settled on a general value of 1.1 as for the RBE ($RBE_{1.1}$). Proton therapy clinics around the world have adapted this ratio in their protocols (Paganetti 2015). The assumption of 1.1 was adapted as a conservative number, even though experimental data have shown that the effect can be higher and is variable within a treatment field (Paganetti 2014).

The RBE can then be multiplied with the physical proton dose to achieve the RBE-weighted dose (or sometimes termed biological dose), which is the dose quantity that is used and reported in clinics:

$$D_{RBE} = D_p \times RBE, \tag{3.4}$$

To distinguish the difference from physical dose, the unit Gy(RBE) is used for RBE-weighted dose (Durante 2014). The most distinct variation in RBE and RBE-weighted dose is seen along the treatment depth, as qualitatively illustrated by the spread-out Bragg peak (SOBP) example in Figure 5.

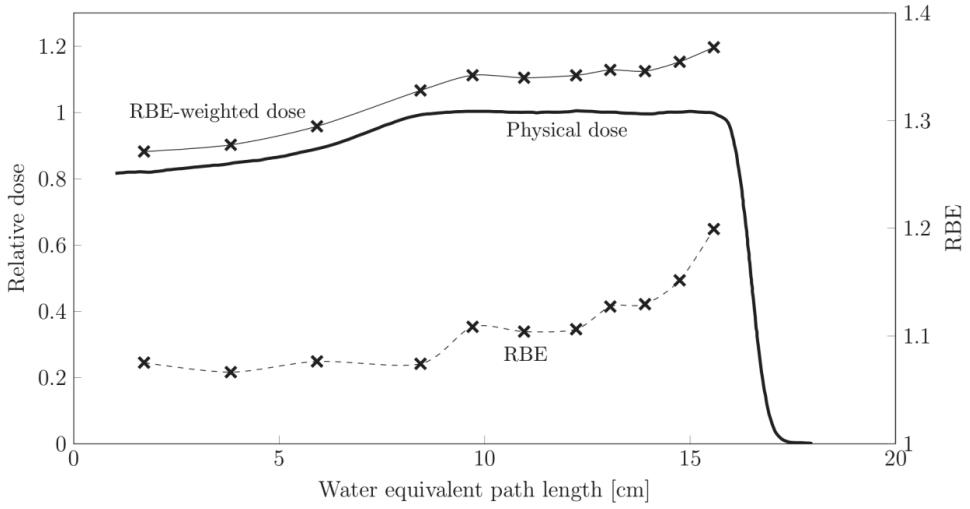

Figure 5: An example of a physical depth dose distribution for a SOBP, found by Monte Carlo simulations. The RBE-weighted dose is plotted above the physical dose, indicating the higher effectiveness for protons over photons, both corresponding to the left axis. The variable RBE value is shown by the

points and the dashed curve. The lines between the points are only for guidance. As seen, the RBE is therefore not constant but increasing with depth in this example. Data extracted from Wouters et al. (2015) and Polster et al. (2015).

The increased RBE with increasing depth is especially an issue for the organs at risk (OARs) distal to the target volume. This increased biological dose to OARs may increase the normal tissue complication probability (NTCP) of a patient treatment, even though the dose constraints are met with the $RBE_{1.1}$ proton therapy plan (Jones 2016).

3.3 Biological modelling of protons

Better understanding of the proton RBE can give more precise treatment and ultimately a reduction in treatment complications. RBE modelling for protons is therefore a subject of high interest, and multiple models have been developed in the recent years.

3.3.1 RBE models in literature

RBE models found in literature can be divided into three major groups: Phenomenological models, plan-based models and mechanistic models.

Phenomenological models try to describe the relationship of measurable empirical quantities (Belli, Campa, and Ermolli 1997, Wilkens, J J and Oelfke 2004, Tilly et al. 2005, Chen and Ahmad 2012, Carabe et al. 2012, Wedenberg, Lind, and Hårdemark 2013, Jones 2015a, 2015b, McNamara, Schuemann, and Paganetti 2015, Mairani et al. 2017, Peeler et al. 2016). The models do not include any information or assumptions of cells on a subcellular level. Instead, the models rely on measurable input and output variables of cell irradiation experiments, typically the LET_d and α and β of experiments. The model creators then assume appropriate dependencies for the model functions with free fitting parameters and perform regression analysis to the data to determine the parameters. This is covered in depth by this thesis.

Plan-based models were developed as an alternative to the phenomenological and mechanistic models and are not directly based on cell experiments (Frese et al. 2011, Unkelbach et al. 2016). The term “plan-based model" is made to make the distinction that the model is made based on information from treatment plans, such as dose and

LET_d distributions. Instead of being based on empirical cell data, the model creators assumed that the average RBE inside the target volume is 1.1, while the variable model functions are normalised to this.

The last group of models are fundamentally different from the other two kind of models, as mechanistic models aim to model the biological effects on a microscopic scale within the cells, not only assuming and calculating relationship between experimental variables (Scholz et al. 1997, Hawkins 1994, Carlson et al. 2008, Cunha et al. 2017, McMahon et al. 2017). The microscopic dose distribution will give rise to lesions and local events within the nucleus, such as double strand breaks (DSB), which are estimated by the models. These events are quantified and used in the estimation of overall cell survival.

The radiosensitivity of the cells is also known to vary with the oxygen level, as hypoxic cells are normally more radioresistant, both for photon and proton radiation (Hall and Giaccia 2006). Specialised models that incorporate the oxygen enhancement ratio (OER) have been developed (Durante 2014), which include the spatial oxygen level as input data. The developed proton RBE models do not consider effects of hypoxia.

3.3.2 Mathematical model functions

The RBE can be coupled with the LQ-model by inserting the mathematical description of the LQ-model of the proton and photon irradiation, as given in Equation (3.1, into Equation (3.3):

$$e^{-(\alpha D_p+\beta {D_p}^2)} = e^{-(\alpha_x D_x+\beta_x {D_x}^2)}, \tag{3.5}$$

where D_p is the physical proton dose, α_x and β_x are the LQ-parameters of the photon radiation, is the physical proton dose and the α and β values are the LQ-parameters of the proton radiation. This equation can be solved for D_x and inserted into the definition of RBE, as given in Equation (3.2:

$$RBE\left[D_p, \alpha, \alpha_x, \beta, \beta_x\right] = \frac{1}{2D_p}\left(\sqrt{\left(\frac{\alpha_x}{\beta_x}\right)^2 + 4D_p\frac{\alpha_x}{\beta_x}\frac{\alpha}{\alpha_x} + 4D_p^2\frac{\beta}{\beta_x}} - \frac{\alpha_x}{\beta_x}\right). \tag{3.6}$$

The RBE of the proton beam is then only a function of the proton dose and the LQ-model parameters. As a general rule, the RBE is highest at low doses and decreases with increasing dose. By evaluating the equation at the proton dose extremes, we achieve two equations for RBE values for either very low doses (RBE_{max}) or high doses (RBE_{min}):

$$\lim_{D_p \to 0} RBE = RBE_{max} = \frac{\alpha}{\alpha_x} \text{ and } \lim_{D_p \to \infty} RBE = RBE_{min} = \sqrt{\beta/\beta_x}, \quad (3.7)$$

As seen, the extremes are simply the ratios (or square root of the ratio) of the LQ-model parameters of the photon and proton radiation. Equation (3.6 can be reformulated with respect to RBE_{max} and RBE_{min}:

$$RBE = \frac{1}{2D_p}\left(\sqrt{\left(\frac{\alpha}{\beta}\right)_x^2 + 4D_p\left(\frac{\alpha}{\beta}\right)_x RBE_{max} + 4{D_p}^2 RBE_{min}^2} - \left(\frac{\alpha}{\beta}\right)_x\right), \quad (3.8)$$

where $(\alpha/\beta)_x$, equivalent to α_x/β_x, is the treatment fractionation sensitivity of the reference radiation.

In principle, all phenomenological proton RBE models created up to this date can be parametrised into describing the two RBE extrema, even though the models are derived and modelled from different principles. The models will differ in how RBE_{max} and RBE_{min} are defined and on which input parameters the models are made dependent. It should be mentioned that some models quantify the α and β model parameters instead of RBE_{max} and RBE_{min}, however, these are closely linked to each other by Equation (3.7. One generic example for both RBE_{max} and RBE_{min} are given in Figure 6, where the equations are made linearly dependent on the LET_d value. For a specific dose value, the RBE is found between these two lines, depending on both the dose deposited and the LET_d values of the protons.

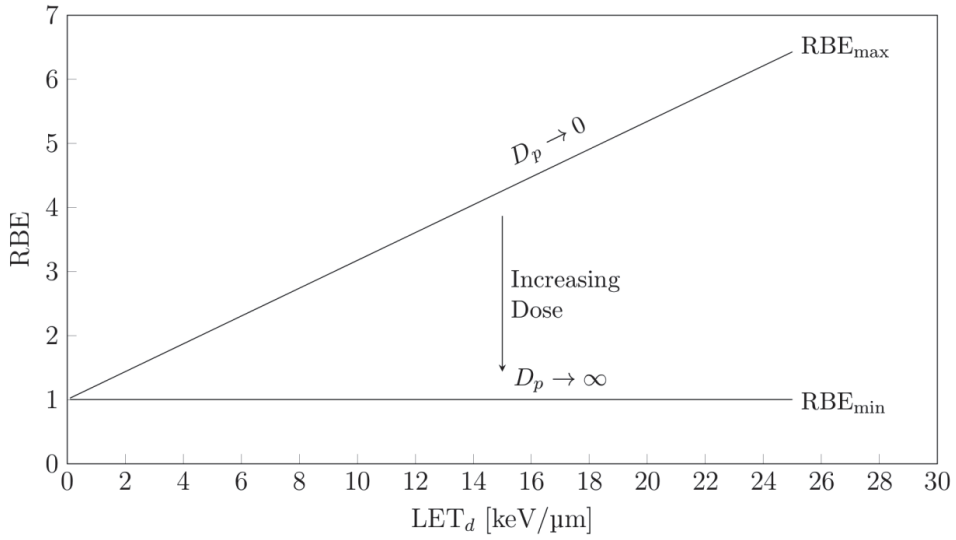

Figure 6: An illustration of two model functions for RBE_{max} and RBE_{min} where the RBE_{max} always is greater than RBE_{min}. For a specific physical fraction dose, the resulting RBE is found somewhere in between the two extreme functions.

3.3.3 RBE dependencies

The variable RBE models for proton therapy can be made dependent on three major parameters: The physical proton dose per fraction, radiation quality and tissue type (Paganetti 2014). The dose dependency is covered by the dose input in Equation (3.8, as RBE_{max} and RBE_{min} are independent on the fraction dose.

An example of the variation in RBE with radiation quality can be seen in Figure 7 for one cell line. The steepness of the curves increases with increasing LET_d value. Therefore, a proton beam with a higher LET_d value will reach a chosen survival fraction at a lower dose compared to a beam with a lower LET_d. This means that the RBE is positive dependent on the LET_d value. It is therefore typical to incorporate the increase in RBE with increasing LET_d in RBE models, at least for the RBE_{max}, as illustrated in the generic example of Figure 6.

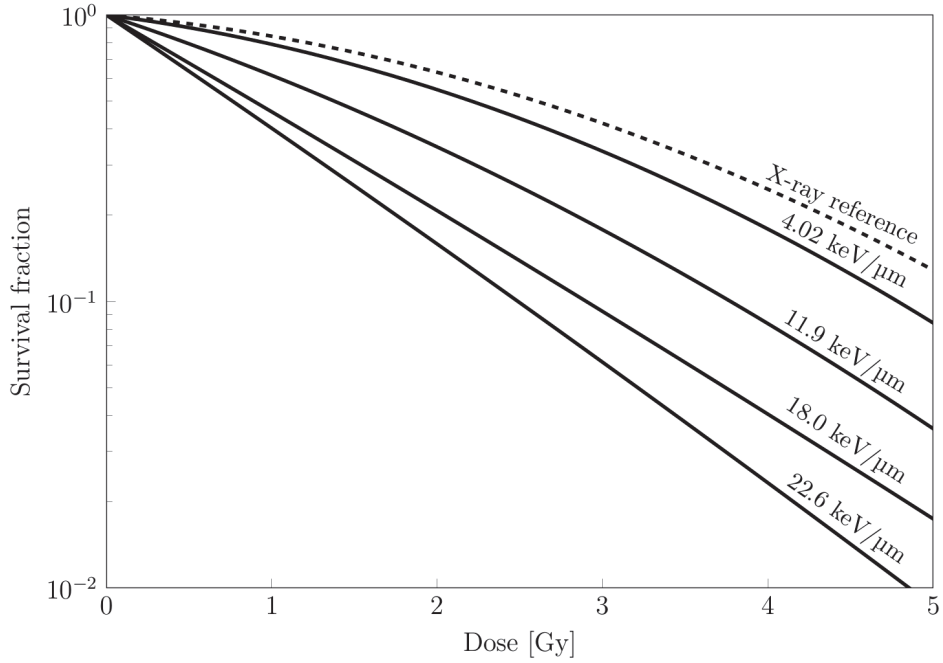

Figure 7: Schematic dose response curves of irradiated U87 cells, irradiated with monoenergetic protons with the noted LET_d values or with X-rays as reference radiation. The α and β data originates from Chaudhary et al. (2014).

The RBE also varies with different tissue types and cell lines. Survival curves for five cell lines irradiated with approximately the same LET_d value are shown in Figure 8A, with the LET_d dependency of RBE_{max} of the cell lines shown in Figure 8B. The large variation between the cell lines, advocates the inclusion of a tissue dependency in RBE models. For modelling proposes, the tissue or cell line is commonly represented by the $(\alpha/\beta)_x$ value. It has been shown both analytically and experimentally, that RBE_{max} is inversely dependent on the $(\alpha/\beta)_x$ value (Hawkins 1994, Wedenberg, Lind, and Hårdemark 2013).

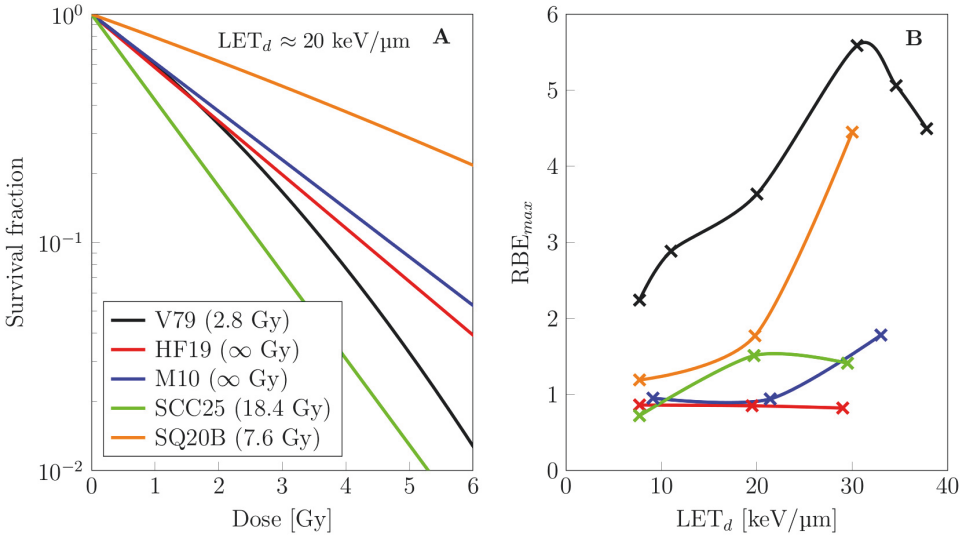

Figure 8: Cell survival curves of five different cell lines, irradiated with monoenergetic protons with approximately 20 keV/µm (A). The RBE$_{max}$ of the same cell lines relative to the LET$_d$ value of the experiments. The lines are only shown for guidance. The lines in A corresponds to the points in the middle of figure B. Data from Belli et al. (1998) and Belli et al. (2000).

3.3.4 Mixed field radiation

As described in section 2.3.1, a clinical beam does not consist of only monoenergetic protons of a single energy, a fact that needs to be taken into consideration when RBE models are created. To simplify the calculation of the RBE from the protons with a wide range of energies and LET values, the LET_d of the total beam is most commonly used as input. This is mathematically correct if the biological weighting functions are linear, thus the model functions can be simplified to be LET_d dependent:

$$RBE_{max}(LET_d) = a + bLET_d \tag{3.9}$$

and

$$RBE_{min}(LET_d) = c + dLET_d, \tag{3.10}$$

where a, b, c and d are model constants, determined by the model creators (Paganetti 2018, Paganetti et al. 2019a). Models with a linear LET dependency enables estimation of the RBE based only on the dose and LET_d distributions. The estimation of RBE and RBE-weighted dose with the help of Equations (3.9) and (3.10) can be performed

subsequent to the dose calculation, a method termed offline calculation (Polster et al. 2015).

Equations (3.9) and (3.10) do, however, only approximate the correct RBE if the LET dependency of the model functions are linear. The approach of using LET_d as a parameter might induce increased uncertainty in the RBE estimates, as some information about the radiation quality of the beam is lost when averaging the spectrum (Grassberger and Paganetti 2011, Inaniwa et al. 2015). If we assume that the LET dependency is non-linear, the equations need to be generalised. The RBE from a mixed field can be regarded as the dose weighted sum of individual RBE components, as earlier showed by Lam (1987). The formula for the mixed RBE can be parameterised into:

$$RBE_{mix}\big(d(L)\big) = \int_0^\infty r(L)\, d(L)\, dL, \tag{3.11}$$

where $\mathrm{r(L)}$ is a LET dependent biological weighting function and $d(\mathrm{L})$ is the dose weighted LET spectrum. As shown by Kanai et al. (1997) and others, the general formula can be separated into the extreme RBE functions:

$$RBE_{max}\big(d(L)\big) = \int_0^\infty \alpha(L)/\alpha_x\, d(L)\, dL = \int_0^\infty r_{max}(L)\, d(L)\, dL \tag{3.12}$$

and

$$RBE_{min}\big(d(L)\big) = \int_0^\infty \sqrt{\beta(L)/\beta_x}\, d(L)\, dL = \int_0^\infty r_{min}(L)\, d(L)\, dL, \tag{3.13}$$

where $\mathrm{r}_{max}\mathrm{(L)}$ and $\mathrm{r}_{\min}\mathrm{(L)}$ are the LET dependent biological weighting functions. It can be shown that Equations (3.9) and (3.10) are specific versions of Equations (3.12) and (3.13) if the biological weighting functions $\mathrm{r}_{max}\mathrm{(L)}$ and $\mathrm{r}_{\min}\mathrm{(L)}$ are linear dependent on the LET value. If a model includes a biological weighting function with a non-linear LET dependency, these equations are obligatory. The RBE estimation then requires the whole LET spectrum as input. This further requires the LET spectrum to be found for every spatial location, if the RBE where to be calculated offline. Alternatively, Equations (3.12) and (3.13) can be estimated during the dose calculation, referred to as online calculation of the RBE-weighted dose (Polster et al. 2015). In

online calculations the RBE model need to be implemented into the software before the dose calculation is performed.

4. Thesis Objective

The overall objective of this thesis was to investigate and improve phenomenological modelling of RBE for proton therapy. This comprised of analysis of existing models, methodology and available experimental data, as well as development of a new phenomenological RBE model. The specific objectives of each paper are given in the following.

Paper I:

- To review the published phenomenological and plan-based RBE models and compare their underlying experimental background and dependencies.
- To create a general formalism for the RBE models and implement them into MC based architecture with a comparison of the resulting RBE-weighted doses to clinical cases.

Paper II:

- To investigate the LET dependency of RBE of cell survival experiments and test if a non-linear dependency will give a better representation of the existing data than a linear dependency.
- To formulate a tissue dependent phenomenological model based on the LET spectrum as a parameter for the radiation quality.

Paper III:

- To aid the creation of RBE models by extracting more data from published experimental data.
- To test how the dose range in the experimental data impact the resulting models.

5. Materials and Methods

5.1 Creation of RBE models from experimental data

Based on previously published models, we devised a standardised routine for creation of phenomenological RBE models for proton therapy, as summarised in the flowchart in Figure 9. All models were made from an experimental database, normally gathered from a literature search with one or several inclusion and exclusion criteria (Figure 9, Box 1a). Some model creators modified and standardised the database before the fitting (Figure 9, Box 1b). The decision on dependencies of the model functions were formulated by the model creators before fitting, often as an educated guess based on the experimental database or inspired by previous publications (Figure 9, Box 2). The fitting of the functions to the database is done by regression to the database (Figure 9, Box 3) and the coefficients are numerically determined (Figure 9, Box 4).

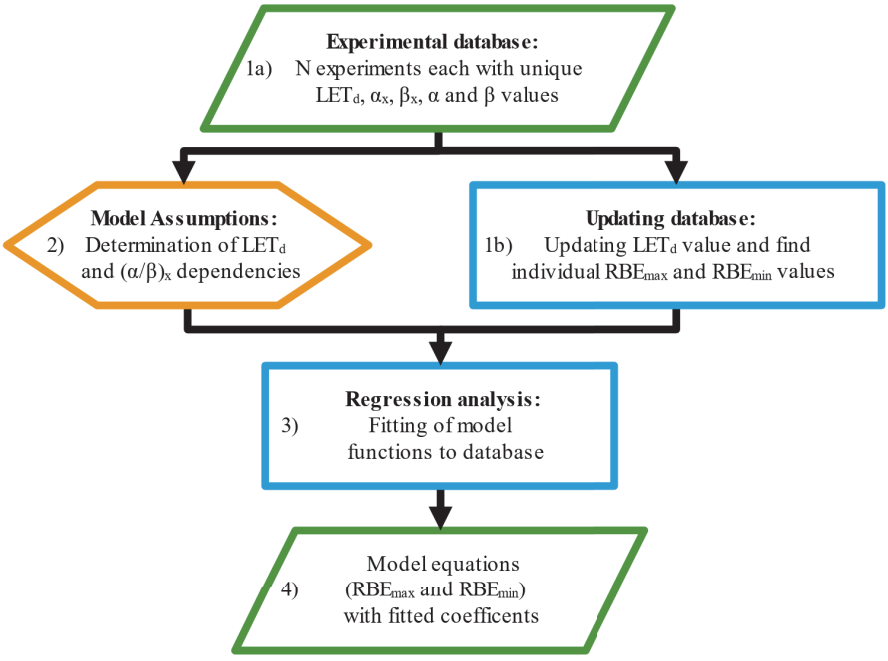

Figure 9: Flow chart of the creation of phenomenological RBE models based on the LQ-model formalism. The green parallelograms describe the input and output, the blue rectangles the calculation processes and the yellow hexagon describe regression preparations.

5.1.1 Experimental database

For Papers II and III, we collected all proton cell survival experiments performed and published up to the time of writing the manuscripts. The extensive literature search was primarily based on the comprehensive database included in the review paper by Paganetti (2014), and complemented by more recent publications.

For both these studies, we only analysed monoenergetic experiments, excluding cells irradiated with an SOBP beam or laser accelerated protons. In Paper II, all LET_d values were allowed, while experiments above 20 keV/µm were excluded in Paper III. The model developed in Paper II was configured for a wide range of cell types, however, experiments with very high $(\alpha/\beta)_x$ values (above 25 Gy) were excluded. Only late responding cells were analysed in Paper III, therefore the exclusion criterium was set to be maximum 5 Gy.

From the included experiments, we extracted the reported LET_d values. Further, the reported LQ-model parameter values were used in Paper II, while for Paper III, we extracted the dose/survival data points from all relevant experiments and refitted the LQ-model to the data points. The refitting was only done for the proton experiments, while the reference photon experiments were kept the same. The database in Paper III was further used as a basis to construct multiple restricted databases, with constraints on the minimum dose followed by refitting of the LQ-model.

After extracting the data from the experiments in Paper II and III, we updated the databases (Figure 9, Box 1b). First, we adjusted for different radiation qualities of the reference radiation by calculating the relative LET_d* (Paganetti 2014, Mairani et al. 2016b). We also found the RBE_{max} and RBE_{min} of every experiment and determined the uncertainty of these quantities. The errors were found by using Gauss error propagation principle from the values and uncertainties in α, β, α_x and β_x. The origins of the uncertainties in α, β, α_x and β_x differs from publication to publication, however, most studies only report the uncertainties found from the regression analysis of the data points.

We did not create a new model or estimate the trend in RBE_{max} and RBE_{min} in Paper I for a specific database. For this study, we found all phenomenological models for the proton RBE published to this date. We further explored all the experimental databases used in the models and compared these to each other, with respect to their LET_d and $(\alpha/\beta)_x$ distributions. We also refitted some of the model functions to the model databases, to check the consequence of excluding outliers from the database.

5.1.2 Model assumptions

In Paper II, we fitted multiple potential functions for the RBE_{max} to the defined database to test the linearity assumption of RBE models. We assumed that the experiments were performed with monoenergetic beams, such that the beam only consisted of protons with a LET value equal to the reported LET_d value. The cell response of the experiment corresponded to the specific LET value L, and the effect of monoenergetic protons can be extrapolated to a mixed field beam with multiple energies. Based on this assumption, we created a biological weighting function ($r_{max}(L)$) based on Equation (3.12, which can be determined by regression to the monoenergetic database:

$$r_{max}(L) = 1 + \frac{\mathrm{Gy}}{(\alpha/\beta)_x}(a_1 L + a_2 L^2 + a_3 L^3 + a_4 L^4 + a_5 L^5), \qquad (5.1)$$

where a_1, a_2, a_3, a_4 and a_5 are coefficents determined by the regression analysis. The higher order terms were excluded from the regression when fitting the lower order polynomials. The function is inversely dependent on the $(\alpha/\beta)_x$ value, similar to other modern models (Wedenberg, Lind, and Hårdemark 2013).

In the creation of the model(s) in Paper II, we assumed that the RBE_{min} is constant and equal to 1 for all LET_d values, which is the most common assumption for RBE_{min} in phenomenological RBE models (Wedenberg, Lind, and Hårdemark 2013, Chen and Ahmad 2012, Wilkens, J J and Oelfke 2004). This assumption was tested in Paper III, by introducing a linear function with only the first order coefficient *c* as a free fitting parameter:

$$RBE_{min} = 1 + cLET_d, \qquad (5.2)$$

where c was found from linear regression to each of the restricted database. Only RBE_{min} was estimated in Paper III, not RBE_{max}.

5.1.3 Regression analysis

In both Paper II and Paper III, the RBE_{max} and RBE_{min} functions were found by unweighted and weighted regression. For the latter, the inverse of the uncertainty of RBE_{max} and RBE_{min} were used as weights.

A more complex function will naturally fit better to the data, however, increasing the polynomial order may lead to overfitting (Hawkins 2004, Friedrich 2016). A Chi-squared test was used in Paper II to decide the superior fit. The test rejected the lower order polynomial, if the results gave a p-value under 0.05 (95% confidence level), which indicate that the extra parameters result in a better fit without overfitting.

In Paper III regression was performed in two separate procedures: As described in section 5.1.1, the LQ-model was first fitted to the dose/survival data points, and these parameters were used in the experimental database. Subsequently, the function in Equation (5.2) was fitted to the restricted databases to determine the single c parameter. If the fitting interval of c did not include 0, we regarded the RBE_{min} function to be independent on the LET_d value.

5.2 Recalculation of treatment plans

Today in proton therapy, no treatment planning systems (TPS) includes a standard option to estimate the LET_d or the RBE-weighted dose (D_{RBE}) with a variable RBE model. In order to quantify the RBE and D_{RBE} for clinical treatment plans we used the FLUKA Monte Carlo code (Böhlen et al. 2014, Ferrari et al. 2005) to estimate the RBE. In Paper I, we compared the RBE-modelled dose for all phenomenological models, both in a water phantom and for clinical cases. In Paper II, we compared our own developed RBE-model to the models by Wedenberg et al. (2013) and McNamara et al. (2015) for a SOBP in a water phantom.

All treatment plans were created in a clinical TPS (Varian Eclipse™ (Varian Medical Systems, Palo Alto, California)) and imported into the FLUKA/Flair architecture by a locally developed software solution (Fjæra et al. 2017). All the SOBP plans were

optimised with a single field to give a uniform dose across the target volume, while the patient plans were planned with two treatment fields.

Within the FLUKA architecture, the CT images of the patient were imported and transformed to the FLUKA geometry with Flair, a graphical user interface software for FLUKA. The system had previously been calibrated to the Eclipse™ TPS to give an acceptable and comparable proton range for every relevant energy and material (Fjæra et al. 2017). In FLUKA, so-called subroutines are used for complex simulations not achievable through standard source definition and scoring. Two subroutines were modified to calculate the dose.

First, the *source* subroutine was adapted to simulate all the pencil beams with the internal distribution. Based on their weighting, the properties (energy, spot position, beam focus) of each primary proton was randomly sampled from the distribution of pencil beams. Each pencil beam was defined by its position and energy. The SOBP plans were calculated with 100 million primary protons, while each field of the clinical plans were simulated with 50 million protons.

Further, a *fluscw* (FLUence SCoring Weight) subroutine was also used to score the dose to water (D^w), the $LET_d{}^w$ and the D_{RBE}. This was done in an identical grid to the scoring matrix of the prefabricated plan made by the TPS, thus keeping the same resolution. For a single particle, the fluence-like quantity of a single particle can be estimated by finding the infinitesimal length of the particle trajectory, divided by infinitesimal volume (Papiez and Battista 1994):

$$\theta_i = \frac{\mathrm{d}l_i}{\mathrm{d}V}. \tag{5.3}$$

The subroutine can modify the spatial scoring, by weighting the spatial fluence (θ_i) of a particle i in the individual voxel by a user defined quantity (W), before it is summed together with the total spatial scored quantity:

$$Scoring = \sum_i W_i \times \theta_i, \tag{5.4}$$

For every voxel, the total scored quantity will be summed over for all particles i passing through. To obtain dose to water for each particle *i*, Equation (5.4 was modified to score:

$$D^w = \sum_i \frac{1}{\rho^w} LET_i^w \times \theta_i, \tag{5.5}$$

where ρ^w is the density of water, LET_i^w is the LET to water of particle *i* and θ_i is the "fluence-like" quantity scored by the traversing particles. The LET^w value of the particle traversing the voxel was obtained with the GETLET() function, included in FLUKA. The function is dependent the particle type, energy and type of material, and it outputs the LET by a lookup table. In our work, we have used the LET from all particles when calculating the full physical dose. Equation (5.5) was also modified to only score the dose to water by protons and deuterium ions, ignoring heavier ions and other particles.

Scoring of LET_d^w was performed in two steps. First the dose to water times the LET_d^w was scored:

$$LET_d^w D^w = \sum_i \frac{1}{\rho^w} (LET_i^w)^2 \times \theta_i. \tag{5.6}$$

The division of $LET_d^w D^w$ by D^w to find LET_d^w was done subsequently in an offline Python script (Fjæra et al. 2017). For all pure proton RBE models, we only estimated the dose deposited and LET value of protons, deuterium ions and tritium ions, both primary and secondary. For all LET_d based models, this quantity was used to find the RBE_{max} and the RBE_{min} for every model. Subsequently, these quantities were used together with the spatial distributed D_i^w values to find the RBE_i values by Equation (3.8.

For RBE models based on the energy and LET spectrum, the RBE_{max} and RBE_{min} quantities had to be calculated online during the simulations. This was also done by the *fluscw* subroutine by finding the quantities multiplied by the dose and dividing with the dose offline. The quantities were found based on Equations (3.12) and (3.13):

$$RBE_{max}D^w = \sum_i r_{max}\frac{1}{\rho^w}LET_i^w \times \theta_i \tag{5.7}$$

and

$$RBE_{min}D^w = \sum_i r_{min}\frac{1}{\rho^w}LET_i^w \times \theta_i, \tag{5.8}$$

where r_{max} and r_{min} are the biological weighting functions defined by each RBE model.

All these quantities are scored in a volume, estimated from the track length of the particles in a grid of voxel volumes. While for the SOBP examples, we scored the full LET spectrum (d(L)) directly from planes perpendicular to the beam axis with the USRYIELD (USeR defined YIELD) scoring card. The spectrum was defined as a histogram of 1000 bins, logarithmic spaced between 0.01 keV/µm and 100 keV/µm for every 0.5 mm along the depth of the phantom. The LET_d and the RBE and D_{RBE} of the models where all found in a MATLAB analysis architecture offline, subsequent the simulations.

6. Summary of Results

6.1 Paper I: Comparison of phenomenological models

Paper I include a wide comparison of all phenomenological models for the proton RBE that were published before November 2017, as well as two plan-based models leading to an investigation of in total 14 models. For all models the RBE values increased with increasing LET_d value and depth, as seen in Figure 10. The extent of the RBE varied with the models and the RBE-weighted doses ranged, in some extreme cases, from 28-52 Gy(RBE). This indicates that the selection of RBE model in a dose planning study is highly significant.

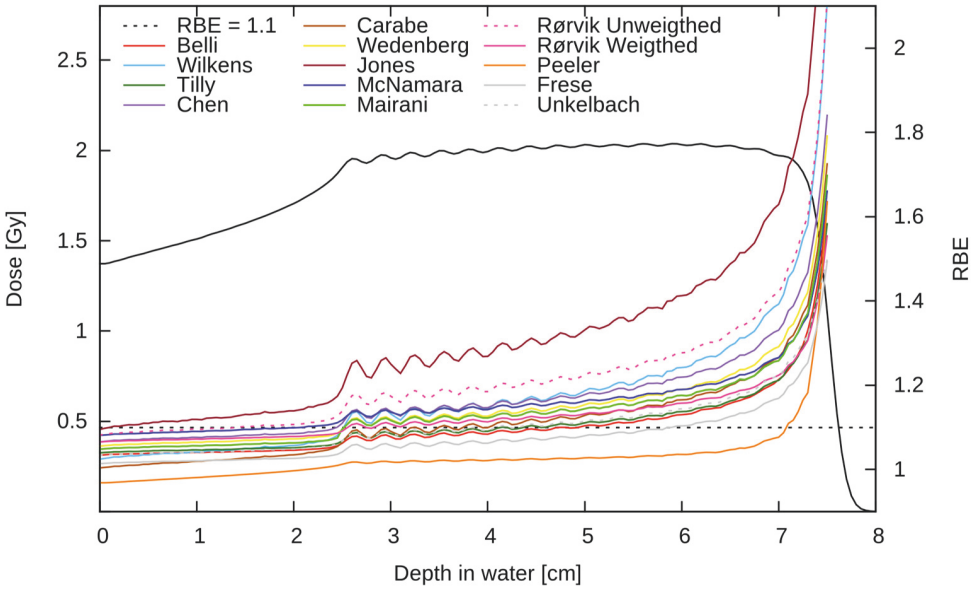

Figure 10: A depth distribution of a SOBP in water. The physical dose is shown by the black line, corresponding to the left y-axis and the estimated RBE values from all models are shown by the coloured lines corresponding to the right y-axis.

The differences in RBE could be traced back to the fundamental definition of the RBE model functions, RBE_{max} and RBE_{min}. The comparison showed that the functions mainly diverged by three major reasons: the experimental database of the model, the dependency assumptions of the model functions and the regression technique. The

model databases varied with respect to the distribution and range of LET_d values and reference radiation fractionation sensitivity ($(\alpha/\beta)_x$). The model functions also varied in their different dependencies, based on the assumptions made by the model authors. This is the main reason why some models are made dependent on the $(\alpha/\beta)_x$ value, while other models estimate a constant RBE for all tissue types. Lastly, the regression techniques also differed, mainly as some models used weighted regression with respect to the experimental uncertainty, such that experiments with low uncertainty are preferred over the other. Most models did, however, not include the uncertainties in the LQ-model parameters and used unweighted regression.

6.2 Paper II: LET spectra based model

Two of the models covered in the model study in Paper I (Rørvik unweighted and Rørvik weighted) were developed in Paper II. All phenomenological RBE models for protons developed up to the time of writing had assumed that the RBE-LET relationship was linear, an assumption we wanted to test. The paper introduces the mathematical formalism to incorporate the LET spectrum in phenomenological models, which could also be used in future models. In our literature search, we found 85 monoenergetic experiments fulfilling our database constraints. The statistical test determined which of the five polynomials fitted to the database gave the best fit.

The results showed that the relationship might be non-linear if the database was weighted relative to the measurement uncertainty with a quartic function as shown in Figure 11. The non-linear shape of the weighted RBE_{max} function is relatively flat until 10 keV/µm, where the function increases drastically. This means in practice that monoenergetic beams with LET_d around 5-10 keV/µm will give a relatively low RBE value, while a proton beam with many energies with similar LET_d values typically found at the end of a poly-energetical SOBP, would give higher values. If all the experiments in the database were instead considered equal and an unweighted method was applied, RBE_{max} would be linear.

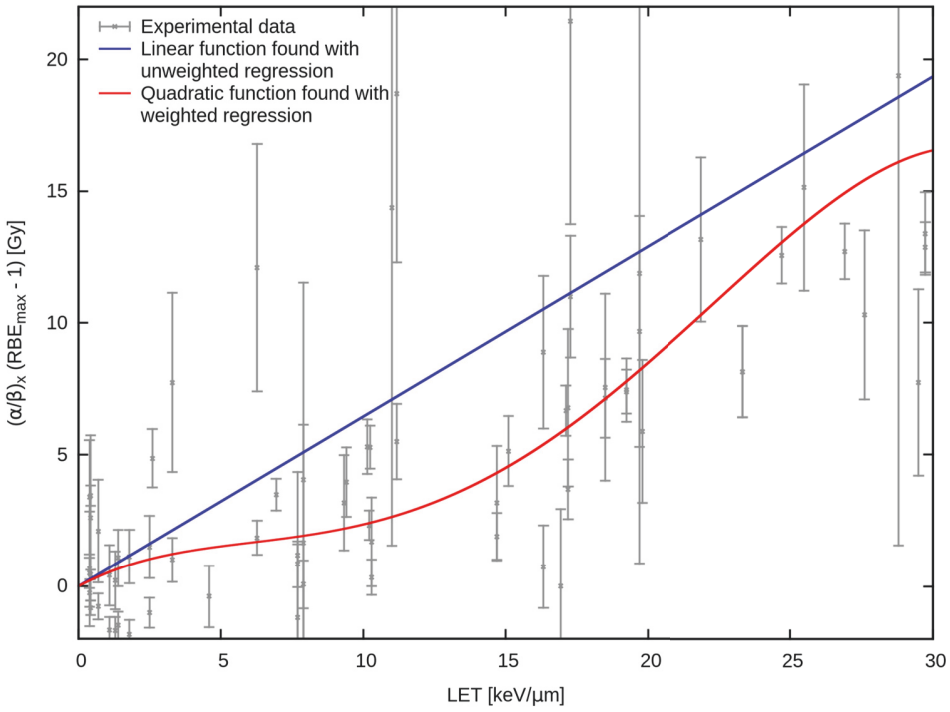

Figure 11: The experimental database used in the modelling shown in grey and the superior polynomial. The expression used in this figure ($(\alpha/\beta)_x(RBE_{max} - 1)$) is a substitute for the RBE_{max} value, independent on the $(\alpha/\beta)_x$ value of the experiments, enabling 2D illustration and analysis of the LET dependency.

For all clinically relevant LET_d values, the unweighted method gave a higher RBE_{max} value compared to the weighted method. In the SOBP example included in the paper, the weighted model gave relatively similar RBE values to models made by Carabe et al. (2012), McNamara et al. (2015) and Wedenberg et al. (2013), with a mean RBE of 1.14 across the SOBP, while the unweighted gave a significant higher value of 1.22.

6.3 Paper III: The dose dependency of RBE_{min}

Paper III address the issue of creating a phenomenological model from a database of multiple experiments from different publications and connecting it to the variation in RBE_{min} by modifying the database constraints. The resulting variation in the RBE_{min} function can be seen in Figure 12, where the *c* value is the first order coefficient in

Equation (5.2). In those cases where c equals 0, the RBE_{min} function is considered constant, which is seen in the figure for high D_η values i.e. high minimum dose in the restricted database.

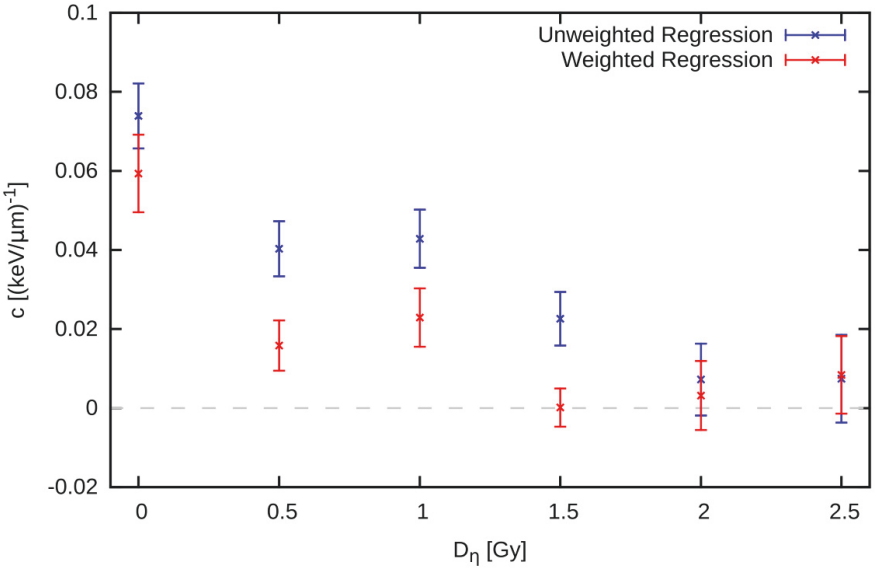

Figure 12: The evolution of the c parameter, the first order coefficient of the LET_d dependent RBE_{min} function. The D_η value correspond to the minimum dose of the restricted database. As seen, the c parameter decreases with increasing minimum dose, until around 2 Gy.

Our results for both weighted and unweighted regression revealed the RBE_{min} to be constant for databases with high minimum doses, i.e. 2 Gy or higher. By including low dose data in the LQ-model regression, the RBE_{min} can be regarded as variable and increasing with increasing LET_d value, as seen in Figure 12. A database based on a low minimum dose will then give an RBE_{min} of 1.4±0.1 for a LET_d value around of 5 keV/µm, while databases with only high dose data (> 2 Gy) gave an RBE_{min} of 1.0±0.1. None of our restricted databases gave a decreasing RBE_{min} with increasing LET_d, in contrary to some of the phenomenological and mechanistic RBE models. Applying a constant RBE_{min} equal to 1 might underestimate the RBE.

7. Discussion

The published phenomenological models deviate in the RBE-weighted dose estimations. As we have shown, the models vary in the definition of the RBE_{max} and RBE_{min} functions, which originate from different decisions in the construction of databases, model assumptions and regression techniques. The variations in the databases can be seen by the database distribution illustrations shown in Paper I and the effect of database variations are also demonstrated in the RBE_{min} function with variable minimum dose in Paper III. The great variation in the estimated RBE-weighted doses indicate that it is not irrelevant which model that is chosen in a dose planning study. These results indicate that users of RBE models should make their choice of model based on the underlying database and assumptions, suitable to the specific use.

The statistical analysis in Paper II indicate that the LET-RBE_{max} relationship is non-linear. This is in contrast to the established and recognised linear dependency assumed and applied in most proton RBE models (Paganetti 2015). Simultaneous to the publication of Paper II, Mairani et al. also tested this assumption (Mairani et al. 2017). The statistical analysis of their work did, however, conclude that a linear dependency was sufficient. Mairani et al. used the same experimental publications as was used in the database applied in the model by Wedenberg et al. (2013), however, they also included experiments with LET_d value above 30 keV/µm, adding 6 experiments to the database up to 37.8 keV/µm. Our differences in the conclusions could be traced back to differences in the database construction. As shown in Paper I, the database in our work was significantly greater, with 85 experiments. Specially, our database also included the 24 experiments done by Guan et al. (2015a), which showed a clear non-linear LET-RBE_{max} relationship. The experiment was reproduced at another location, also showing indications of a non-linear LET-RBE_{max} relationship (Patel et al. 2017).

The investigation in Paper II expanded the use of LET spectrum as an input for phenomenological models. Since the publication of the paper, Grün et al. have investigated the use of LET spectrum instead of the LET_d value in the Local Effect

Model (LEM) (Grün et al. 2019). The LEM model has a clear non-linear RBE_{max} function, with a super linear dependency around 5 keV/µm, in agreement with our weighted model. Grün et al conclude that a model cannot be based on the LET_d value if there is a clear non-linear dependency, this should also be true for our phenomenological approach.

The uncertainty in the RBE value can be lowered by gaining more knowledge and creating better and more precise models. The work done in this thesis, by including the full LET spectrum or the dose dependency of the experimental data, might be a stepping stone for the creation of other novel models, increasing the precision of the RBE estimations.

7.1 Experimental databases

For our modelling work in Paper II and III, we collected data from multiple experimental groups and arranged them together in a large database with different experiments. The creation of databases from different papers and labs could be problematic, as the various experiments have different setups and protocols. Differences in the biological lab work, such as the chemicals used and cell counting methods applied might also cause a difference between the experiments (Guan et al. 2015a). The publications may include and report different errors or correct the experiments for different effects (Paganetti 2014). Recently, two guides on reporting of experimental data have been published, which could contribute to more coherent methods in future experiments (Paganetti et al. 2019b, Durante et al. 2019).

For the work in this thesis, experiments executed with a SOBP beam or laser accelerated protons were excluded, as these result in a wide LET spectrum for each radiation quality of the experiments. In Paper II, we practically assumed that the LET spectra for all our experiments were very narrow, such that they formed a perfect delta function around the LET_d value. This assumption could lead to inaccuracies in the modelling, especially for low energetic protons with high LET_d value from a degraded high energy beam, as the range straggling effect widen the spectrum (Guan et al.

2015a). Additionally, some inconsistencies in the LET_d value could be caused by different LET estimation methods, as some groups have only found the LET value from analytical models based on the remaining range or energy (Belli et al. 1993), while other have found this from comprehensive Monte Carlo calculations (Dahle et al. 2017). A longer discussion on the estimation and reporting of LET value is given in section 7.4.

The regression of the LQ-model could also cause variations, if it is fitted to the linear or logarithmic survival data, or whether it is done with a weighted or unweighted regression technique, as we investigated in Paper III, illustrated in Appendix A1 of the paper. In this paper, the associated interlaboratory error was minimised, as we fitted the LQ-model directly to the dose-survival data in a coherent manner. It could be debated that our unweighted regression to the logarithmic data is suboptimal compared to weighted regression, however, it was impossible to extract the uncertainties from the various experiments.

7.2 Assumptions made for RBE_{max} and RBE_{min}

The general dependencies of the RBE_{max} and RBE_{min} functions are determined by the model authors before fitting to the database. Ideally, the models should be as independent of the authors as possible to minimise the impact of researcher bias. This can be done by introducing multiple assumptions and let statistical analysis decide which assumptions that best describe the database, as was done in Paper II and other models (Mairani et al. 2017, Wedenberg, Lind, and Hårdemark 2013).

For paper III we only included a linear LET dependency of the RBE_{min} function since our goal was to test the common assumption of a constant RBE_{min}, independent of the LET_d value. In this work, we excluded an $(\alpha/\beta)_x$ dependency on RBE_{min} by only including experiments with low $(\alpha/\beta)_x$ values in our database. From the analysis in Paper I, the $(\alpha/\beta)_x$ dependency of RBE_{min} deviated for the different models, either linearly dependent on the $(\alpha/\beta)_x$ value (Peeler 2016), the square root of the $(\alpha/\beta)_x$ value

(McNamara, Schuemann, and Paganetti 2015) or the inverse of the $(\alpha/\beta)_x$ value (Carabe et al. 2012). The $(\alpha/\beta)_x$ dependency of RBE_{min} should therefore be investigated further.

7.3 Regression techniques

In Paper I, we revealed that model functions were usually created by regression analysis of fitting functions with free variables, either by unweighted regression or weighted regression where the variations in uncertainties in the database are considered. For our own model in Paper II and the analysis in Paper III, we used both regression methods. As shown in Figure 11 and by the regression results in Paper II, the choice of method has a significant impact. Generally speaking, one would assume that the weighted technique would give the best representation of the database. Weighted regression can be beneficial when the experimental database is unequally sampled, since it can reduce the bias due to outliers with large uncertainties. This is given under the assumption that there is a coherent reporting of the uncertainty in experiments, which is not the case in the existing experiments (Paganetti et al. 2019b).

It is also possible to create RBE_{max} and RBE_{min} functions by other methods than statistical regression. As shown in Paper I, Belli et al. created the functions by linear interpolations in between the experimental data points (Belli, Campa, and Ermolli 1997). Mairani et al. also tested an alternative to the RBE_{min} function by having a running average (Mairani et al. 2017). Machine learning techniques could also be applied to find dependencies in the database. If full LET spectrum data extracted from the experiments will be reported in the future, as discussed in recent reviews (Durante et al. 2019, Paganetti et al. 2019b), spectral unfolding techniques could alternatively be used to find the best fitting model functions (Reginatto 2010). As our investigations in Paper I shows, most models can be described by simple functions with one to four coefficients. However, the model by Belli et al. (1997) is an noticeable exeption, as it is defined by a table to find the corresponding RBE_{max} and RBE_{min} values for a given energy. The use of tables instead of explicit functions is already common for mechanistic models (Stewart et al. 2018), and it could also be applied in new phenomenological models.

7.4 Software implementations

Over the recent years, multiple Monte Carlo based software solutions have been developed with the possibility to recalculate patient plans with biological dose estimation (Böhlen et al. 2014, Ferrari et al. 2005, Polster et al. 2015). We used the FLUKA Monte Carlo code to estimate the dose and RBE in this thesis, as it enables a wide range of possibilities and ability to score various quantities. Other software architectures have been developed to specifically estimate the LET_d and RBE distribution of a proton plan. Some of these implementations are based on fast and simplified Monte Carlo algorithms (Ödén, Eriksson, and Toma-Dasu 2017a, Kohno et al. 2019), while other are based on analytical LET_d algorithms (Choi et al. 2018, Wieser et al. 2017). Even though they are faster than a full Monte Carlo simulation, the user should be aware of the limitations, as precision is traded against calculation time. With regard to our work in Paper I, only full Monte Carlo software like FLUKA is able to produce the full LET spectra today, which is needed for the input. Creating an analytical algorithm for the full LET spectrum for a TPS should be feasible, based on simplified rules for range straggling and nuclear interactions.

Spectrum based models need to be implemented directly into the software and calculated online during the dose calculation. In practice, this means that model functions need to be defined before the calculation, together with all relevant $(\alpha/\beta)_x$ values and variations of the model coefficients. Offline calculation only estimates the pure physical quantities (dose and LET values) and offer the possibility to adjust the physical values after the patient plan have been calculated. This can be convenient for analysis of various models' coefficients and some robust planning procedures. Furthermore, typical offline analysis of the uncertainty of RBE models similar to the work by Ödén et al (2017b) is not straight forward for spectrum based models.

In our calculations, we estimated the LET value with two different methods, either volumetrically or across boundaries (Guan et al. 2015b). Ideally, the LET should be scored in a grid equal to the dose grid, so the LET value needs be scored volumetrically. Volumetric scoring also enables more precise scoring from multiple fields with

different angles. Only the LET to water was scored in this work, instead of LET to tissue. Dose to water is standardised to report in radiotherapy (Liu, Keall, and Hendee 2002). It is therefore natural that the equivalent is also reported for LET, even though it can differ significantly from LET to tissue, and might exclude some effects, especially within the lungs and bone (Wilkens, Jan J. and Oelfke 2004).

In our calculations, we used the LET value from only protons, both primary and secondary protons, which is typical for other studies as well (Yepes et al. 2019, Granville and Sawakuchi 2015, Wilkens and Oelfke 2003). However, other secondaries could also affect the LET value (Grassberger and Paganetti 2011). According to a recent study, the variation from including or excluding heavier ions might be large and could double the LET_d value (Grzanka, Ardenfors, and Bassler 2018). A method to include the effect of various particles into a single RBE estimate have been integrated in the phenomenological model by Mairani (Mairani et al. 2017, 2016a, 2016b) or for many mechanistic models (Stewart et al. 2018).

7.5 Suggestions to experimental reporting

The reported quantities in phenomenological models should ideally be similar, both for the reported experimental data and application to clinical cases. The dose and LET value of the experiment should be calculated in the same manner as the use in patient calculations, with the same definitions of the scored LET, with regard to the material and energy cut off value. The dose levels of experiments should also be covering a greater range of values, especially including low doses under 1 Gy, as these values are clinically relevant for OARs in normal fractionated proton plans. As we showed in Paper III, many experiments are, however, lacking data for dose levels under 1 Gy.

As recently suggested by the work groups on RBE experiments (Durante et al. 2019, Paganetti et al. 2019b), the full LET spectrum from experiments could be reported. Some recent articles have included experiments and analysis of wide and narrow spectra with the same LET_d value (Chaudhary et al. 2014, Howard et al. 2018, Grün et al. 2019, Dahle et al. 2017), however, all of these only give an illustration of the spectra.

As it is not possible or convenient to report full spectra numerically in conventional articles, it could be possible that the data is uploaded directly into an online database, like the Particle Irradiation Data Ensemble (Friedrich et al. 2013). This could both help create more precise models and verify the precision of existing models. Further, such a database could also include all the individual dose-survival data points from the experiment including uncertainties, not only the commonly reported α and β values. This will aid projects like the work in Paper III, as we had to extract data from figures, instead of the directly measured data. It could also enable easier adaptation and development of the novel global fitting method, as described by Abolfath et al. (2017). This method fit both the RBE_{max} and RBE_{min} functions simultaneous and directly to the experimental survival data in one single regression, instead of conventional approach of one regression of the LQ-model followed by another fit for each of the two model functions.

7.6 The effect of variable RBE

A variable RBE can be beneficial, if the increased effect of protons is located at the tumour location. This aspect could be quantified by the ratio of RBE-weighted dose to the tumour and the normal tissue, i.e. the biological effective dose ratio (BEDR) (Holzscheiter et al. 2006, Grün et al. 2015). A higher BEDR value correspond to a better treatment effect and is preferred for optimal treatment. An increased BEDR is the reason why heavier ions, like helium ions and carbon ions are considered extra effective compared to protons, as shown in a comparison by Jäkel (2006, 2009).

From Paper I we see that most models estimate an increasing RBE value with increasing LET_d value, decreasing $(\alpha/\beta)_x$ value and decreasing physical proton dose, similar to the conclusions given by Paganetti in a review paper of experimental data (Paganetti 2014). The LET_d value is higher in the tumour than the normal tissue in front of the tumour, leading to a generally greater BEDR value. However, this is only valid with the assumption of similar $(\alpha/\beta)_x$ for the tumour and normal tissues. With higher $(\alpha/\beta)_x$ for the tumour, the predicted BEDR will be reduced. The BEDR will therefore be highly case specific.

7.7 Is an RBE of 1.1 still an appropritate assumption?

In this work, we have only reanalysed existing experimental data in the literature. Most of the cells included in our analysis in Paper II and III are from Chinese hamsters and other animals (Paganetti 2014). This could introduce an uncertainty in biological response, as these cell lines could divert from the spontaneous human tumours. Phenomenological models could then be based solely on cultivated normal cells from human tissue, estimating the RBE for normal tissue or solely on human cancer cells for the RBE to the target (Hall et al. 1988, Belli et al. 2000).

In vitro experiments and analysis of cell irradiations is perhaps not enough alone to challenge the established assumption of a constant RBE of 1.1. There should at least be relevant *in vivo* data, from irradiation of rats and mice, proving that there is a non-negligible variable RBE in proton therapy that needs to be accounted for. A meta-analysis of existing *in vivo* data from 2002 found no significant variation in the RBE and ratified the use of a constant RBE of 1.1 (Paganetti et al. 2002). However, more recent experiment work on animal models, irradiated with multiple LET_d values, have indeed indicated that there is a correlation between increased LET and RBE (Sørensen et al. 2017, Saager et al. 2018, Szabó et al. 2018).

Although a variable RBE has been seen in preclinical experiments, there has not been documented an increased rate of clinical complications in treated patients which can be traced back to an increased RBE above 1.1 (Lühr et al. 2018, Paganetti 2015). This still advocates for keeping a constant RBE in clinical protocols (Paganetti 2015). However, a recent study investigating MR images of the brain post treatment, found a correlation between increased LET values and image changes (Peeler et al. 2016). Another study also found image changes in the chest wall of lung, which could be related to increased LET values (Underwood et al. 2018). The clinical consequences for the patients with these image changes are still unknow, and longer follow up time is needed to determine if they lead to complications. Nevertheless, proton therapy clinics should still consider the potential risk in treatment planning by carefully selecting the treatment fields to spare OARs of possible high RBE values (Paganetti et al. 2019b).

8. Conclusion

The transfer from conventional radiotherapy with photons to modern radiotherapy with protons is not only a change in the physical dose deposition, but also in the biological response of the ionising radiation. The RBE concept enables easy transition of existing photon therapy protocols to be used in proton therapy. In this thesis, possible alternatives to the generic use of constant RBE have been investigated, through analysis and development of phenomenological models from cell survival databases.

Large deviations between different RBE models were found in the estimations of the RBE-weighted dose. The dissection and parameterisation of the models traced the differences in the estimation to the variations in database distributions of $(\alpha/\beta)_x$ values and LET_d values, model assumptions and regression technique.

The LET dependencies for both RBE_{max} and RBE_{min} were further investigated. To explore non-linear models, the full LET spectrum was implemented as input in phenomenological RBE models. Based on a large database of all published cell survival experiments with monoenergetic protons and statistical analysis, a weighted regression analysis indicated that the LET-RBE_{max} relationship is indeed non-linear, contrary to other established models. By extracting the dose-survival data from a large database of experiments on late responding cells, the LET_d-RBE_{min} relationship was studied with a novel two step regression analysis method. The examination of restricted databases of experiments with a minimum dose at 1 Gy or lower indicated that the RBE_{min} function increases with increasing LET_d value.

Overall, the thesis shows similarities and differences between existing phenomenological RBE models for proton therapy and show multiple possibilities of developing novel model by reanalysing existing experimental data that can challenge common assumptions in the RBE dependencies and give a better understanding of the biological differences between photon therapy and proton therapy.

References

Abolfath, R., Peeler, C.R., Newpower, M., Bronk, L., Grosshans, D., and Mohan, R. (2017) 'A Model for Relative Biological Effectiveness of Therapeutic Proton Beams Based on a Global Fit of Cell Survival Data'. *Scientific Reports* 7 (1), 8340

Barton, M.B., Jacob, S., Shafiq, J., Wong, K., Thompson, S.R., Hanna, T.P., and Delaney, G.P. (2014) 'Estimating the Demand for Radiotherapy from the Evidence: A Review of Changes from 2003 to 2012'. *Radiotherapy and Oncology* 112 (1), 140–144

Belli, M., Bettega, D., Calzolari, P., Cera, F., Cherubini, R., Dalla Vecchia, M., Durante, M., Favaretto, S., Gialanella, G., Grossi, G., Marchesini, R., Moschini, G., Piazzola, A., Poli, G., Pugliese, M., Sapora, O., Scampoli, P., Simone, G., Sorrentino, E., Tabocchini, M.A., Tallone, L., and Tiveron, P. (2000) 'Inactivation of Human Normal and Tumour Cells Irradiated with Low Energy Protons'. *International Journal of Radiation Biology* 76 (6), 831–839

Belli, M., Campa, A., and Ermolli, I. (1997) 'A Semi-Empirical Approach to the Evaluation of the Relative Biological Effectiveness of Therapeutic Proton Beams: The Methodological Framework'. *Radiation Research* 148 (6), 592–598

Belli, M., Cera, F., Cherubini, R., Dalla Vecchia, M., Haque, A.M., Ianzini, F., Moschini, G., Sapora, O., Simone, G., Tabocchini, M.A., and Tiveron, P. (1998) 'RBE-LET Relationships for Cell Inactivation and Mutation Induced by Low Energy Protons in V79 Cells: Further Results at the LNL Facility'. *International Journal of Radiation Biology* 74 (4), 501–509

Belli, M., Cera, F., Cherubini, R., Haque, A.M.I., Ianzini, F., Moschini, G., Sapora, O., Simone, G., Tabocchini, M.A., and Tiveron, P. (1993) 'Inactivation and Mutation Induction in V79 Cells by Low Energy Protons: Re-Evaluation of the Results at the LNL Facility'. *International Journal of Radiation Biology* 63 (3), 331–337

Bernard Gottschalk (2011) 'Physics of Proton Interactions in Matter'. in *Proton Therapy Physics* [online] Series in Medical Physics and Biomedical Engineering. 0 vols. CRC Press, 19–60. available from <http://www.crcnetbase.com/doi/abs/10.1201/b11448-3> [21 June 2015]

Bethe, H. (1930) 'Zur Theorie Des Durchgangs Schneller Korpuskularstrahlen Durch Materie'. *Annalen Der Physik* 397 (3), 325–400

Bethe, H.A. (1953) 'Molière's Theory of Multiple Scattering'. *Physical Review* 89 (6), 1256–1266

Bloch, F. (1933a) ‘Bremsvermögen von Atomen mit mehreren Elektronen’. *Zeitschrift für Physik* 81 (5), 363–376

Bloch, F. (1933b) ‘Zur Bremsung Rasch Bewegter Teilchen Beim Durchgang Durch Materie’. *Annalen Der Physik* 408 (3), 285–320

Böhlen, T.T., Cerutti, F., Chin, M.P.W., Fassò, A., Ferrari, A., Ortega, P.G., Mairani, A., Sala, P.R., Smirnov, G., and Vlachoudis, V. (2014) ‘The FLUKA Code: Developments and Challenges for High Energy and Medical Applications’. *Nuclear Data Sheets* 120, 211–214

Brennsæter, J.A. (2015) ‘The Influence of the Energy Degrader Material for a Therapeutical Proton Beam’. *77* [online] available from <https://brage.bibsys.no/xmlui/handle/11250/2352179> [6 April 2019]

Carabe, A., Moteabbed, M., Depauw, N., Schuemann, J., and Paganetti, H. (2012) ‘Range Uncertainty in Proton Therapy Due to Variable Biological Effectiveness’. *Physics in Medicine and Biology* 57 (5), 1159

Carlson, D.J., Stewart, R.D., Semenenko, V.A., and Sandison, G.A. (2008) ‘Combined Use of Monte Carlo DNA Damage Simulations and Deterministic Repair Models to Examine Putative Mechanisms of Cell Killing’. *Radiation Research* 169 (4), 447–459

Chaudhary, P., Marshall, T.I., Perozziello, F.M., Manti, L., Currell, F.J., Hanton, F., McMahon, S.J., Kavanagh, J.N., Cirrone, G.A.P., Romano, F., Prise, K.M., and Schettino, G. (2014) ‘Relative Biological Effectiveness Variation Along Monoenergetic and Modulated Bragg Peaks of a 62-MeV Therapeutic Proton Beam: A Preclinical Assessment’. *International Journal of Radiation Oncology*Biology*Physics* 90 (1), 27–35

Chen, Y. and Ahmad, S. (2012) ‘Empirical Model Estimation of Relative Biological Effectiveness for Proton Beam Therapy’. *Radiation Protection Dosimetry* 149 (2), 116–123

Choi, K., Mein, S.B., Kopp, B., Magro, G., Molinelli, S., Ciocca, M., and Mairani, A. (2018) ‘FRoG—A New Calculation Engine for Clinical Investigations with Proton and Carbon Ion Beams at CNAO’. *Cancers* 10 (11), 395

Cunha, M., Monini, C., Testa, E., and Beuve, M. (2017) ‘NanOx, a New Model to Predict Cell Survival in the Context of Particle Therapy’. *Physics in Medicine and Biology* 62 (4), 1248

Dahle, T.J., Rykkelid, A.M., Stokkevåg, C.H., Mairani, A., Görgen, A., Edin, N.J., Rørvik, E., Fjæra, L.F., Malinen, E., and Ytre-Hauge, K.S. (2017) ‘Monte Carlo Simulations of a Low Energy Proton Beamline for Radiobiological Experiments’. *Acta Oncologica* 56 (6), 779–786

Durante, M. (2014) 'New Challenges in High-Energy Particle Radiobiology'. *The British Journal of Radiology* 87 (1035), 20130626

Durante, M., Paganetti, H., Pompos, A., Kry, S.F., Wu, X., and Grosshans, D.R. (2019) 'Report of a National Cancer Institute Special Panel: Characterization of the Physical Parameters of Particle Beams for Biological Research'. *Medical Physics* 46 (2), e37–e52

Fano, U. (1953) 'Degradation and Range Straggling of High-Energy Radiations'. *Physical Review* 92 (2), 328–349

Ferrari, A., Sala, P.R., Fasso, A., and Ranft, J. (2005) *FLUKA: A Multi-Particle Transport Code*. CERN-2005-10, INFN/TC_05/11, SLAC-R-773

FHI (2018) *Kreft er nå hyppigste dødsårsak i Norge* [online] available from <http://www.fhi.no/nyheter/2018/dodsarsakene-2017/> [19 March 2019]

Fjæra, L.F., Li, Z., Ytre-Hauge, K.S., Muren, L.P., Indelicato, D.J., Lassen-Ramshad, Y., Engeseth, G.M., Brydøy, M., Mairani, A., Flampouri, S., Dahl, O., and Stokkevåg, C.H. (2017) 'Linear Energy Transfer Distributions in the Brainstem Depending on Tumour Location in Intensity-Modulated Proton Therapy of Paediatric Cancer'. *Acta Oncologica* 56 (6), 763–768

Frese, M.C., Wilkens, J.J., Huber, P.E., Jensen, A.D., Oelfke, U., and Taheri-Kadkhoda, Z. (2011) 'Application of Constant vs. Variable Relative Biological Effectiveness in Treatment Planning of Intensity-Modulated Proton Therapy'. *International Journal of Radiation Oncology*Biology*Physics* 79 (1), 80–88

Friedrich, T. (2016) *Biophysical Modeling of Effects of Ionizing Radiation and Associated Uncertainties* [online] Darmstadt. available from <http://tuprints.ulb.tu-darmstadt.de/6189/>

Friedrich, T., Scholz, U., Elsässer, T., Durante, M., and Scholz, M. (2013) 'Systematic Analysis of RBE and Related Quantities Using a Database of Cell Survival Experiments with Ion Beam Irradiation'. *Journal of Radiation Research* 54 (3), 494–514

Granville, D.A. and Sawakuchi, G.O. (2015) 'Comparison of Linear Energy Transfer Scoring Techniques in Monte Carlo Simulations of Proton Beams'. *Physics in Medicine and Biology* 60 (14), N283

Grassberger, C. and Paganetti, H. (2011) 'Elevated LET Components in Clinical Proton Beams'. *Physics in Medicine and Biology* 56 (20), 6677

Greilich, S., Grzanka, L., Bassler, N., Andersen, C.E., and Jäkel, O. (2010) 'Amorphous Track Models: A Numerical Comparison Study'. *Radiation Measurements* 45 (10), 1406–1409

Grün, R., Friedrich, T., Krämer, M., Zink, K., Durante, M., Engenhart-Cabillic, R., and Scholz, M. (2015) 'Assessment of Potential Advantages of Relevant Ions for Particle Therapy: A Model Based Study'. *Medical Physics* 42 (2), 1037–1047

Grün, R., Friedrich, T., Traneus, E., and Scholz, M. (2019) 'Is the Dose-Averaged LET a Reliable Predictor for the Relative Biological Effectiveness?' *Medical Physics* 46 (2), 1064–1074

Grzanka, L. (2014) 'Modelling Beam Transport and Biological Effectiveness to Develop Treatment Planning for Ion Beam Radiotherapy'. *ArXiv:1410.1378 [Physics]* [online] available from <http://arxiv.org/abs/1410.1378> [21 June 2015]

Grzanka, L., Ardenfors, O., and Bassler, N. (2018) 'Monte Carlo Simulations of Spatial LET Distributions in Clinical Proton Beams'. *Radiation Protection Dosimetry* 180 (1–4), 296–299

Guan, F., Bronk, L., Titt, U., Lin, S.H., Mirkovic, D., Kerr, M.D., Zhu, X.R., Dinh, J., Sobieski, M., Stephan, C., Peeler, C.R., Taleei, R., Mohan, R., and Grosshans, D.R. (2015a) 'Spatial Mapping of the Biologic Effectiveness of Scanned Particle Beams: Towards Biologically Optimized Particle Therapy'. *Scientific Reports* 5, 9850

Guan, F., Peeler, C., Bronk, L., Geng, C., Taleei, R., Randeniya, S., Ge, S., Mirkovic, D., Grosshans, D., Mohan, R., and Titt, U. (2015b) 'Analysis of the Track- and Dose-Averaged LET and LET Spectra in Proton Therapy Using the Geant4 Monte Carlo Code'. *Medical Physics* 42 (11), 6234–6247

Hall, E.J. and Giaccia, A.J. (2006) *Radiobiology for the Radiologist*. Lippincott Williams & Wilkins

Hall, E.J., Marchese, M., Hei, T.K., and Zaider, M. (1988) 'Radiation Response Characteristics of Human Cells in Vitro'. *Radiation Research* 114 (3), 415–424

Hawkins, D.M. (2004) 'The Problem of Overfitting'. *Journal of Chemical Information and Computer Sciences* 44 (1), 1–12

Hawkins, R.B. (1994) 'A Statistical Theory of Cell Killing by Radiation of Varying Linear Energy Transfer'. *Radiation Research* 140 (3), 366–374

Hirayama, R., Ito, A., Tomita, M., Tsukada, T., Yatagai, F., Noguchi, M., Matsumoto, Y., Kase, Y., Ando, K., Okayasu, R., and Furusawa, Y. (2009) 'Contributions of Direct and Indirect Actions in Cell Killing by High-LET Radiations'. *Radiation Research* 171 (2), 212–218

Holzscheiter, M.H., Bassler, N., Agazaryan, N., Beyer, G., Blackmore, E., DeMarco, J.J., Doser, M., Durand, R.E., Hartley, O., Iwamoto, K.S., Knudsen, H.V., Landua, R., Maggiore, C., McBride, W.H., Møller, S.P., Petersen, J., Skarsgard,

L.D., Smathers, J.B., Solberg, T.D., Uggerhøj, U.I., Vranjes, S., Withers, H.R., Wong, M., and Wouters, B.G. (2006) 'The Biological Effectiveness of Antiproton Irradiation'. *Radiotherapy and Oncology* 81 (3), 233–242

Howard, M.E., Beltran, C., Anderson, S., Tseung, W.C., Sarkaria, J.N., and Herman, M.G. (2018) 'Investigating Dependencies of Relative Biological Effectiveness for Proton Therapy in Cancer Cells'. *International Journal of Particle Therapy* [online] available from </doi/abs/10.14338/IJPT-17-00031.1> [19 December 2018]

ICRU (1993) 'ICRU Report 49, Stopping Powers and Ranges for Protons and Alpha Particles'. *International Commission on Radiation Units and Measurements*

ICRU (1970) 'ICRU Report 16, Linear Energy Transfer'. *International Commission on Radiation Units and Measurements*

Inaniwa, T., Furukawa, T., Kase, Y., Matsufuji, N., Toshito, T., Yoshitaka Matsumoto, Furusawa, Y., and Noda, K. (2010) 'Treatment Planning for a Scanned Carbon Beam with a Modified Microdosimetric Kinetic Model'. *Physics in Medicine & Biology* 55 (22), 6721

Inaniwa, T., Kanematsu, N., Matsufuji, N., Kanai, T., Shirai, T., Noda, K., Tsuji, H., Kamada, T., and Tsujii, H. (2015) 'Reformulation of a Clinical-Dose System for Carbon-Ion Radiotherapy Treatment Planning at the National Institute of Radiological Sciences, Japan'. *Physics in Medicine and Biology* 60 (8), 3271

Jäkel, O. (2009) 'Medical Physics Aspects of Particle Therapy'. *Radiation Protection Dosimetry* 137 (1–2), 156–166

Jäkel, O. (2006) 'Heavy Ion Radiotherapy'. in *New Technologies in Radiation Oncology* [online] ed. by Schlegel, W., Bortfeld, T., and Grosu, A.-L. Medical Radiology. Berlin, Heidelberg: Springer Berlin Heidelberg, 365–377. available from <https://doi.org/10.1007/3-540-29999-8_28> [22 March 2019]

Jermann, M. (2018) *PTCOG - Patient Statistics* [online] available from <https://ptcog.ch/index.php/patient-statistics> [29 March 2019]

Joiner, M.C. and Kogel, A. van der (2016) *Basic Clinical Radiobiology, Fifth Edition*. CRC Press

Jones, B. (2016) 'Why RBE Must Be a Variable and Not a Constant in Proton Therapy'. *The British Journal of Radiology* 20160116

Jones, B. (2015a) 'A Simpler Energy Transfer Efficiency Model to Predict Relative Biological Effect for Protons and Heavier Ions'. *Frontiers in Oncology* [online] 5. available from <http://www.ncbi.nlm.nih.gov/pmc/articles/PMC4531328/> [18 April 2017]

Jones, B. (2015b) 'Towards Achieving the Full Clinical Potential of Proton Therapy by Inclusion of LET and RBE Models'. *Cancers* 7 (1), 460–480

Kanai, T., Furusawa, Y., Fukutsu, K., Itsukaichi, H., Eguchi-Kasai, K., and Ohara, H. (1997) 'Irradiation of Mixed Beam and Design of Spread-Out Bragg Peak for Heavy-Ion Radiotherapy'. *Radiation Research* 147 (1), 78–85

Kaplan, H.S. and Moses, L.E. (1964) 'Biological Complexity and Radiosensitivity'. *Science* 145 (3627), 21–25

Kohno, R., Cao, W., Yepes, P., Bai, X., Poenisch, F., Grosshans, D.R., Akimoto, T., and Mohan, R. (2019) 'Biological Dose Comparison between a Fixed RBE and a Variable RBE in SFO and MFO IMPT with Various Multi-Beams for Brain Cancer'. *International Journal of Medical Physics, Clinical Engineering and Radiation Oncology* 08, 32

Lam, G.K.Y. (1987) 'The Survival Response of a Biological System to Mixed Radiations'. *Radiation Research* 110 (2), 232–243

Liu, H.H., Keall, P., and Hendee, W.R. (2002) 'Dm Rather than Dw Should Be Used in Monte Carlo Treatment Planning'. *Medical Physics* 29 (5), 922–924

Loncol, T., Cosgrove, V., Denis, J.M., Gueulette, J., Mazal, A., Menzel, H.G., Pihet, P., and Sabattier, R. (1994) 'Radiobiological Effectiveness of Radiation Beams with Broad LET Spectra: Microdosimetric Analysis Using Biological Weighting Functions'. *Radiation Protection Dosimetry* 52 (1–4), 347–352

Lühr, A., von Neubeck, C., Krause, M., and Troost, E.G.C. (2018) 'Relative Biological Effectiveness in Proton Beam Therapy – Current Knowledge and Future Challenges'. *Clinical and Translational Radiation Oncology* 9, 35–41

Lühr, A., Toftegaard, J., Kantemiris, I., Hansen, D.C., and Bassler, N. (2012) 'Stopping Power for Particle Therapy: The Generic Library LibdEdx and Clinically Relevant Stopping-Power Ratios for Light Ions'. *International Journal of Radiation Biology* 88 (1–2), 209–212

Mairani, A., Dokic, I., Magro, G., Tessonnier, T., Bauer, J., Böhlen, T.T., Ciocca, M., Ferrari, A., Sala, P.R., Jäkel, O., J Debus, Haberer, T., Abdollahi, A., and Parodi, K. (2017) 'A Phenomenological Relative Biological Effectiveness Approach for Proton Therapy Based on an Improved Description of the Mixed Radiation Field'. *Physics in Medicine and Biology* 62 (4), 1378

Mairani, A., Dokic, I., Magro, G., Tessonnier, T., Kamp, F., Carlson, D.J., Ciocca, M., Cerutti, F., Sala, P.R., Ferrari, A., Böhlen, T.T., Jäkel, O., Parodi, K., Debus, J., Abdollahi, A., and Haberer, T. (2016a) 'Biologically Optimized Helium Ion Plans: Calculation Approach and Its in Vitro Validation'. *Physics in Medicine and Biology* 61 (11), 4283

Mairani, A., Magro, G., Dokic, I., Valle, S.M., Tessonnier, T., Galm, R., Ciocca, M., Parodi, K., Ferrari, A., Jäkel, O., T Haberer, Pedroni, P., and Böhlen, T.T. (2016b) 'Data-Driven RBE Parameterization for Helium Ion Beams'. *Physics in Medicine and Biology* 61 (2), 888

Malvezzi, M., Carioli, G., Bertuccio, P., Boffetta, P., Levi, F., La Vecchia, C., and Negri, E. (2018) 'European Cancer Mortality Predictions for the Year 2018 with Focus on Colorectal Cancer'. *Annals of Oncology* 29 (4), 1016–1022

McMahon, S.J., McNamara, A.L., Schuemann, J., Paganetti, H., and Prise, K.M. (2017) 'A General Mechanistic Model Enables Predictions of the Biological Effectiveness of Different Qualities of Radiation'. *Scientific Reports* 7 (1), 10790

McNamara, A.L., Schuemann, J., and Paganetti, H. (2015) 'A Phenomenological Relative Biological Effectiveness (RBE) Model for Proton Therapy Based on All Published in Vitro Cell Survival Data'. *Physics in Medicine and Biology* 60 (21), 8399

Metropolis, N. and Ulam, S. (1949) 'The Monte Carlo Method'. *Journal of the American Statistical Association* 44 (247), 335–341

Molière, G. (1948) 'Theorie Der Streuung Schneller Geladener Teilchen II. Mehrfach- Und Vielfachstreuung'. *Zeitschrift Naturforschung Teil A* 3, 78–97

Newhauser, W.D. and Zhang, R. (2015) 'The Physics of Proton Therapy'. *Physics in Medicine and Biology* 60 (8), R155

Ödén, J., Eriksson, K., and Toma-Dasu, I. (2017a) 'Inclusion of a Variable RBE into Proton and Photon Plan Comparison for Various Fractionation Schedules in Prostate Radiation Therapy'. *Medical Physics* 44 (3), 810–822

Ödén, J., Eriksson, K., and Toma-Dasu, I. (2017b) 'Incorporation of Relative Biological Effectiveness Uncertainties into Proton Plan Robustness Evaluation'. *Acta Oncologica* 0 (0), 1–10

Paganetti, H. (2018) 'Proton Relative Biological Effectiveness – Uncertainties and Opportunities'. *International Journal of Particle Therapy* 5 (1), 2–14

Paganetti, H. (2015) 'Relating Proton Treatments to Photon Treatments via the Relative Biological Effectiveness—Should We Revise Current Clinical Practice?' *International Journal of Radiation Oncology • Biology • Physics* 91 (5), 892–894

Paganetti, H. (2014) 'Relative Biological Effectiveness (RBE) Values for Proton Beam Therapy. Variations as a Function of Biological Endpoint, Dose, and Linear Energy Transfer'. *Physics in Medicine and Biology* 59 (22), R419

Paganetti, H. (2009) ‘Dose to Water versus Dose to Medium in Proton Beam Therapy’. *Physics in Medicine and Biology* 54 (14), 4399–4421

Paganetti, H. (2002) ‘Nuclear Interactions in Proton Therapy: Dose and Relative Biological Effect Distributions Originating from Primary and Secondary Particles’. *Physics in Medicine and Biology* 47 (5), 747

Paganetti, H., Blakely, E., Carabe-Fernandez, A., Carlson, D.J., Das, I.J., Dong, L., Grosshans, D., Held, K.D., Mohan, R., Moiseenko, V., Niemierko, A., Stewart, R.D., and Willers, H. (2019a) ‘Report of the AAPM TG-256 on the Relative Biological Effectiveness of Proton Beams in Radiation Therapy’. *Medical Physics* [online] 0 (0). available from <https://aapm.onlinelibrary.wiley.com/doi/abs/10.1002/mp.13390> [10 March 2019]

Paganetti, H., Blakely, E., Carabe-Fernandez, A., Carlson, D.J., Das, I.J., Dong, L., Grosshans, D., Held, K.D., Mohan, R., Moiseenko, V., Niemierko, A., Stewart, R.D., and Willers, H. (2019b) ‘Report of the AAPM TG-256 on the Relative Biological Effectiveness of Proton Beams in Radiation Therapy’. *Medical Physics* 46 (3), e53–e78

Paganetti, H., Niemierko, A., Ancukiewicz, M., Gerweck, L.E., Goitein, M., Loeffler, J.S., and Suit, H.D. (2002) ‘Relative Biological Effectiveness (RBE) Values for Proton Beam Therapy’. *International Journal of Radiation Oncology*Biology*Physics* 53 (2), 407–421

Papiez, L. and Battista, J.J. (1994) ‘Radiance and Particle Fluence’. *Physics in Medicine and Biology* 39 (6), 1053–1062

Patel, D., Bronk, L., Guan, F., Peeler, C.R., Brons, S., Dokic, I., Abdollahi, A., Rittmüller, C., Jäkel, O., Grosshans, D., Mohan, R., and Titt, U. (2017) ‘Optimization of Monte Carlo Particle Transport Parameters and Validation of a Novel High Throughput Experimental Setup to Measure the Biological Effects of Particle Beams’. *Medical Physics* 44 (11), 6061–6073

Peeler, C.R. (2016) *Assessing the Potential Clinical Impact of Variable Biological Effectiveness in Proton Radiotherapy*.

Peeler, C.R., Mirkovic, D., Titt, U., Blanchard, P., Gunther, J.R., Mahajan, A., Mohan, R., and Grosshans, D.R. (2016) ‘Clinical Evidence of Variable Proton Biological Effectiveness in Pediatric Patients Treated for Ependymoma’. *Radiotherapy and Oncology* 121 (3), 395–401

Polster, L., Schuemann, J., Rinaldi, I., Burigo, L., McNamara, A.L., Stewart, R.D., Attili, A., Carlson, D.J., Sato, T., Méndez, J.R., Faddegon, B., Perl, J., and Paganetti, H. (2015) ‘Extension of TOPAS for the Simulation of Proton Radiation Effects Considering Molecular and Cellular Endpoints’. *Physics in Medicine and Biology* 60 (13), 5053

Quaresma, M., Coleman, M.P., and Rachet, B. (2015) '40-Year Trends in an Index of Survival for All Cancers Combined and Survival Adjusted for Age and Sex for Each Cancer in England and Wales, 1971–2011: A Population-Based Study'. *The Lancet* 385 (9974), 1206–1218

Reginatto, M. (2010) 'Overview of Spectral Unfolding Techniques and Uncertainty Estimation'. *Radiation Measurements* 45 (10), 1323–1329

Saager, M., Peschke, P., Brons, S., Debus, J., and Karger, C.P. (2018) 'Determination of the Proton RBE in the Rat Spinal Cord: Is There an Increase towards the End of the Spread-out Bragg Peak?' *Radiotherapy and Oncology* 128 (1), 115–120

Scholz, M., Kellerer, A.M., Kraft-Weyrather, W., and Kraft, G. (1997) 'Computation of Cell Survival in Heavy Ion Beams for Therapy'. *Radiation and Environmental Biophysics* 36 (1), 59–66

Sørensen, B.S., Bassler, N., Nielsen, S., Horsman, M.R., Grzanka, L., Spejlborg, H., Swakoń, J., Olko, P., and Overgaard, J. (2017) 'Relative Biological Effectiveness (RBE) and Distal Edge Effects of Proton Radiation on Early Damage in Vivo'. *Acta Oncologica* 56 (11), 1387–1391

Stewart, R.D., Carlson, D.J., Butkus, M.P., Hawkins, R., Friedrich, T., and Scholz, M. (2018) 'A Comparison of Mechanism-Inspired Models for Particle Relative Biological Effectiveness (RBE)'. *Medical Physics* 45 (11), e925–e952

Szabó, E.R., Brand, M., Hans, S., Hideghéty, K., Karsch, L., Lessmann, E., Pawelke, J., Schürer, M., and Beyreuther, E. (2018) 'Radiobiological Effects and Proton RBE Determined by Wildtype Zebrafish Embryos'. *PLOS ONE* 13 (11), e0206879

Tilly, N., Johansson, J., Isacsson, U., Medin, J., Blomquist, E., Grusell, E., and Glimelius, B. (2005) 'The Influence of RBE Variations in a Clinical Proton Treatment Plan for a Hypopharynx Cancer'. *Physics in Medicine and Biology* 50 (12), 2765

Tommasino, F. and Durante, M. (2015) 'Proton Radiobiology'. *Cancers* 7 (1), 353–381

Traneus, E. and Ödén, J. (2019) 'Introducing Proton Track-End Objectives in Intensity Modulated Proton Therapy Optimization to Reduce Linear Energy Transfer and Relative Biological Effectiveness in Critical Structures'. *International Journal of Radiation Oncology*Biology*Physics* 103 (3), 747–757

Underwood, T.S.A., Grassberger, C., Bass, R., MacDonald, S.M., Meyersohn, N.M., Yeap, B.Y., Jimenez, R.B., and Paganetti, H. (2018) 'Asymptomatic Late-Phase Radiographic Changes Among Chest-Wall Patients Are Associated With a Proton RBE Exceeding 1.1'. *International Journal of Radiation Oncology • Biology • Physics* 101 (4), 809–819

Unkelbach, J., Botas, P., Giantsoudi, D., Gorissen, B.L., and Paganetti, H. (2016) 'Reoptimization of Intensity Modulated Proton Therapy Plans Based on Linear Energy Transfer'. *International Journal of Radiation Oncology*Biology*Physics* 96 (5), 1097–1106

Wedenberg, M., Lind, B.K., and Hårdemark, B. (2013) 'A Model for the Relative Biological Effectiveness of Protons: The Tissue Specific Parameter α/β of Photons Is a Predictor for the Sensitivity to LET Changes'. *Acta Oncologica* 52 (3), 580–588

Widder, J., van der Schaaf, A., Lambin, P., Marijnen, C.A.M., Pignol, J.-P., Rasch, C.R., Slotman, B.J., Verheij, M., and Langendijk, J.A. (2016) 'The Quest for Evidence for Proton Therapy: Model-Based Approach and Precision Medicine'. *International Journal of Radiation Oncology*Biology*Physics* 95 (1), 30–36

Wieser, H.-P., Cisternas Jimenez, E., Wahl, N., Ulrich, S., Stadler, A., Mescher, H., Müller, L.-R., Klinge, T., Gabrys, H., Burigo, L., Mairani, A., Ecker, S., Ackermann, B., Ellerbrock, M., Parodi, K., Jäkel, O., and Bangert, M. (2017) 'Development of the Open-Source Dose Calculation and Optimization Toolkit MatRad'. *Medical Physics* n/a-n/a

Wilkens, J J and Oelfke, U. (2004) 'A Phenomenological Model for the Relative Biological Effectiveness in Therapeutic Proton Beams'. *Physics in Medicine and Biology* 49 (13), 2811–2825

Wilkens, Jan J. and Oelfke, U. (2004) 'Three-Dimensional LET Calculations for Treatment Planning of Proton Therapy'. *Zeitschrift Für Medizinische Physik* 14 (1), 41–46

Wilkens, J.J. and Oelfke, U. (2003) 'Analytical Linear Energy Transfer Calculations for Proton Therapy'. *Medical Physics* 30 (5), 806–815

Wilson, R.R. (1946) 'Radiological Use of Fast Protons'. *Radiology* 47 (5), 487–491

Wouters, B.G., Skarsgard, L.D., Gerweck, L.E., Carabe-Fernandez, A., Wong, M., Durand, R.E., Nielson, D., Bussiere, M.R., Wagner, M., Biggs, P., Paganetti, H., and Suit, H.D. (2015) 'Radiobiological Intercomparison of the 160 MeV and 230 MeV Proton Therapy Beams at the Harvard Cyclotron Laboratory and at Massachusetts General Hospital'. *Radiation Research* 183 (2), 174–187

Yepes, P., Adair, A., Frank, S.J., Grosshans, D.R., Liao, Z., Liu, A., Mirkovic, D., Poenisch, F., Titt, U., Wang, Q., and Mohan, R. (2019) 'Fixed- versus Variable-RBE Computations for Intensity Modulated Proton Therapy'. *Advances in Radiation Oncology* 4 (1), 156–167

Publications

Graphic design: Communication Division, UiB / Print: Skipnes Kommunikasjon AS

uib.no

ISBN: 9788230854891 (print)
9788230855300 (PDF)